

Applications of Selected Chemical Additives to Decrease Pulp Fibre Network Strength and their Relation to Pipeline Plug Removal in an Industrial Setting

by

Ryan Christensen

BSc (Hons), Medicinal Chemistry, University of New Brunswick, 2016

A Thesis Submitted in Partial Fulfillment of the Requirements for the degree of

Master of Science in Chemical Engineering

in the Graduate Academic Unit of the Department of Chemical Engineering

Supervisor: Yonghao Ni, Ph.D., Chemical Engineering

Examining Board: Felipe Chibante, Ph.D., Chemical Engineering

Guida Bendrich, Ph.D., Chemical Engineering

John Neville, Ph.D., Chemistry

This thesis is accepted by the Dean of Graduate Studies

THE UNIVERSITY OF NEW BRUNSWICK

July, 2019

© Ryan Christensen, 2019

Abstract

A common issue in pulp and paper operations is the blockage of pipelines by plugs of compacted fibre networks, resulting in time consuming and costly procedures being employed for plug removal. A laboratory set-up was established and then used to measure the break-up pressure of fibre-based plugs, which provided an indication of the fibre network strength. Selected chemical additives, namely cupriethylenediamine (CED) and cationic polyacrylamide (C-PAM), were investigated to determine their ability to decrease the fibre network strength and therefore decrease the pressure required for plug removal. The results demonstrated that CED can decrease the network strength through partial fibre dissolution while C-PAM reduces network strength through inter-fibre friction reduction. Both chemical additives have potential to be used in the pulp and paper industry for resolving and/or improving issues arising from fibre-based plugs.

Preface

The research proposal for this work was prepared by my supervisor Prof. Yonghao Ni and Dr. Mark Martinez of The University of British Columbia.

This thesis consists of four chapters. The first introduces the relevant background information, the second and third are versions of separate manuscripts that will be submitted for publication, and the fourth provides conclusions and recommendations.

Chapter 1 provides an in-depth review and critique of selected publications that are relevant to the research topic. Reviewing the literature was a collaborative effort between me, Dr. Wen-Hui Zhang, and Mr. Ryan Lutes. The chapter was written by me, with editorial guidance from Prof. Yonghao Ni.

A version of Chapter 2 will be submitted for publication. The experimental work was a collaborative effort between Dr. Wen-Hui Zhang, me, and Mr. Ryan Lutes. The Manuscript was prepared by me, Dr. Wen-Hui Zhang, Mr. Ryan Lutes, and Prof. Yonghao Ni.

A version of Chapter 3 will be submitted for publication. The experimental work was a collaborative effort between Dr. Wen-Hui Zhang, me, and Mr. Ryan Lutes. The Manuscript was prepared by me, Dr. Wen-Hui Zhang, Mr. Ryan Lutes, and Prof. Yonghao Ni.

Chapter 4 was written by me with editorial guidance from Prof. Yonghao Ni.

Table of Contents

Abstract	ii
Preface.....	iii
Table of Contents.....	iv
List of Figures.....	vii
List of Tables	ix
Nomenclature	x
Acknowledgements.....	xii
1 Introduction	1
1.1 Literature Review	1
1.1.1 Background.....	1
1.1.1.1 Fibre properties and consistency ranges	1
1.1.1.2 Fibre contacts and crowding number	2
1.1.1.3 Forces on fibres and flocculation	4
1.1.2 Yield Stress.....	5
1.1.2.1 Yield stress measurement techniques	5
1.1.2.2 Apparent yield stress findings	6
1.1.3 Fluidization of Pulp Suspensions.....	8
1.1.4 Pulp Suspension Pipe Flow	10
1.1.5 Cellulose Dissolution	12
1.1.5.1 Polymer dissolution	12
1.1.5.2 Cellulose dissolution in NaOH-water systems.....	14
1.1.5.3 Cellulose dissolution in aqueous complexing agents	16
1.1.5.4 Other cellulose solvents	18
1.1.6 Inter-Fibre Frictional Forces.....	19
1.1.6.1 Polymer addition to reduce friction	19
1.1.7 Fibre-Based Pipeline Plugging	20
1.2 Thesis Objectives	21
2 Using Cupriethylenediamine (CED) Solution to Decrease Cellulose Fibre Network Strength for Removal of Pulp Fibre Plugs	22
2.1 Abstract.....	22
2.2 Introduction.....	22

2.3	Materials and Methods	26
2.3.1	Materials	26
2.3.2	Experimental Set-up.....	26
2.3.2.1	Set-up for measuring plug break-up pressure	26
2.3.2.2	Set-up for plug formation.....	29
2.4	Analytical Methods	30
2.4.1	Water Retention Value	30
2.4.2	Mass Loss	30
2.4.3	Degree of Polymerization.....	30
2.4.4	Fibre Properties.....	30
2.4.5	Microscopy Observation	31
2.5	Results and Discussion	31
2.5.1	Plug Break-up Pressure Measurement	31
2.5.2	Effect of Input Pressure Rate.....	32
2.5.3	Effect of Bottom Plate Center Hole Diameter and Plug Mass	33
2.5.4	Effect of CED concentration	34
2.5.5	CED-Assisted De-Plugging Mechanism.....	38
2.6	Conclusions	40
3	Using Cationic Polyacrylamide (C-PAM) Solution to Decrease Cellulose Fibre Network Strength for Removal of Pulp Fibre Plugs.....	41
3.1	Abstract.....	41
3.2	Introduction.....	42
3.3	Materials and Methods	44
3.3.1	Materials	44
3.3.2	Experimental Set-up.....	44
3.3.2.1	Set-up for measuring plug break-up pressure	44
3.3.2.2	Plug formation method	46
3.3.2.3	Break-up pressure measurement.....	46
3.3.3	Analytical Methods.....	46
3.3.3.1	C-PAM adsorption measurement	46
3.4	Results and Discussion	47
3.4.1	Effect of C-PAM Concentration	47
3.4.2	Effect of Reaction Time	51

3.4.3 Effect of Pre-Pressure.....	52
3.4.4 C-PAM Assisted De-Plugging Mechanism.....	53
3.5 Conclusions.....	55
4 Conclusions and Recommendations	56
4.1 Conclusions.....	56
4.2 Recommendations for Future Work.....	57
References	59
Curriculum Vitae	

List of Figures

Figure 1.1. Flow regimes of pulp suspensions.	10
Figure 1.2. Pipe friction loss as a function of flow velocity.	11
Figure 1.3. Schematic diagram of the surface layers formed during polymer dissolution.	14
Figure 1.4. Phase diagram of the cellulose-sodium hydroxide-water system. The triangle encircled in red is the cellulose dissolution zone.	16
Figure 1.5. The proposed structure for dissolved cellulose in an aqueous solution of Pden.....	17
Figure 1.6. Intensive ballooning followed by total dissolution in 0.20 M CED solution.	18
Figure 2.1. Schematic diagram of the experimental set-up for measuring the plug break-up pressure.....	28
Figure 2.2. Cartoon diagram of experimental set-up for measuring the plug break-up pressure.	28
Figure 2.3. Typical pressure signal for determining the plug break-up pressure for the de-plugging trials.	32
Figure 2.4. Effect of input pressure rate on break-up pressure.	33
Figure 2.5. Break-up pressure as a function of plug mass at constant initial plug consistency for two different center hole diameters.	34
Figure 2.6. Effect of CED concentration on break-up pressure for a plug mass of 3.85 g and a 10-minute reaction time.	35
Figure 2.7. Optical microscopy images of original and CED-treated pulp fibres.	37
Figure 2.8. The mechanisms through which CED solution affects fibre network strength.	39
Figure 3.1. Schematic diagram of the experimental set-up for measuring the plug break-up pressure.....	45
Figure 3.2. Cartoon diagram of the experimental set-up for measuring the plug break-up pressure.	45
Figure 3.3. Break-up pressure for different C-PAM concentrations and pulp fibre types (initial pulp consistency: 15 wt.%; reaction time: 30 min).	47
Figure 3.4. Effect of C-PAM concentration on break-up pressure and C-PAM adsorption. (initial pulp consistency: 35 wt.%; mixing time: 5 min (for adsorption measurement); reaction time: 30 min (for break-up pressure measurement)).	50

Figure 3.5. Effect of reaction time on plug break-up pressure at different C-PAM concentrations (initial pulp consistency: 35 wt.%)..... 51

Figure 3.6. The effect of pre-pressure and reaction time on break-up pressure (initial pulp consistency: 35 wt.%) 53

List of Tables

Table 2.1. Change in fibre properties from various 10-minute CED treatments.	36
---	----

Nomenclature

Roman Letters

a	Constant (Pa)
b	Constant (-)
C_m	Mass consistency (%)
C_s	Sediment concentration (%)
DP	Degree of polymerization (-)
D_R	Rotor diameter (m)
D_T	Outer housing diameter (m)
h_L	Pipe friction loss (Pa/m)
LN	Numerical average length (mm)
LW	Length-weighted average fibre length (mm)
LWW	Weight-weighted average fibre length (mm)
M_p	Plug mass (g)
N	Crowding number (-)
N_G	Gel crowding number (-)
P_b	Break-up pressure (psi)
T_g	Glass transition temperature (°C)
V	Flow velocity (m/s)
WRV	Water retention value (g/g)

Greek Letters

ε_f	Power dissipation per unit volume (w/m ³)
η	TAPPI viscosity (cp)
μ	Friction coefficient (-)
σ_y	Yield Stress (Pa)
ω	Fibre coarseness (kg/m)

Abbreviations

BHK	Bleached hardwood Kraft
CED	Cupriethylenediamine
CMC	Carboxymethyl cellulose
C-PAM	Cationic – polyacrylamide
DAQ	Data acquisition
FQA	Fibre quality analyser
NBSK	Northern bleached softwood Kraft
NMMO	N-methylmorpholine-N-oxide
PEO	Polyethylene oxide
UV-Vis	Ultraviolet – visible
WSP	Water soluble polymer

Acknowledgements

I offer my sincere appreciation and thanks to my thesis supervisor Prof. Yonghao Ni for his continual guidance, support, and insightful scientific advice. His commitment and passion for the research at the Limerick Pulp and Paper Centre make it an excellent environment to learn and grow in.

I would like to thank all the students, visiting scholars, and workers at the Pulp and Paper Centre that I have had the privilege to learn from and befriend. More specifically, thank you to Dr. Wen-Hui Zhang, Mr. Ryan Lutes, and Mr. Jinli Zhang, who worked closely and tirelessly along side me in the experimental and writing stages of this work.

To my girlfriend, Katherine Carrier, I thank you for your unconditional support, friendship, and interest in my work. Your empathy and caring throughout this experience have helped me immeasurably.

Finally, to my parents and brothers, who have supported and helped me throughout my entire life, I thank you dearly. I would not be here without you.

1 Introduction

1.1 Literature Review

1.1.1 Background

1.1.1.1 Fibre properties and consistency ranges

Cellulose, which is the most abundant organic polymer on earth, is a linear polysaccharide made of several hundreds to several thousands of $\beta(1\rightarrow4)$ linked D-glucose units. It is one of the three main components of biomass, the other two being hemicellulose and lignin, and is also found in other organisms such as algae and certain types of bacteria.

Pulp is a fibrous material prepared by the mechanical or chemical separation of cellulose from its biomass source. The specific composition of pulp will depend on the pulping methods used for its preparation, however, in general the major constituent of pulp is cellulose and the minor is hemicellulose. Pulp fibres typically have a length of approximately 1 – 3 mm and a diameter of 15 – 30 μm . However, these values differ considerably among species, for example, hard wood fibres have an average length of 1 mm, while soft wood fibres are, on average, significantly longer at 3 mm. Furthermore, significant variability in fibre physical properties, such as length, thickness, and coarseness, exists even for fibres derived from the same biomass source. Because of this variability it is common to express a given fibre property as a weighted average. For example, length weighted average gives more weight to fibres which are longer.

Mass consistency, C_m , often simply called consistency, is defined as the mass of oven-dried fibres divided by the total mass in the suspension. Typically expressed as a

percentage, consistency can be thought of as the mass fraction of the suspension that is composed of solid contents (dry fibres).

In early work, Kerekes et al. [1] classified pulp suspensions in terms of consistency as follows: low consistency ($C_m = 0 - 8\%$), in which the suspension is a water-fibre mixture; medium consistency ($C_m = 8 - 20\%$), obtained by dispersing a mat formed from the vacuum filtration of a low consistency suspension; high consistency ($C_m = 20 - 40\%$), formed by mechanically pressing water from a medium consistency suspension; and ultra-high consistency ($C_m > 40\%$), formed via evaporative drying. In the low consistency range, the suspension is a two-phase slurry consisting of fibres and water. At medium to ultra-high consistencies, the suspension becomes a heterogeneous mixture composed of fibres, water, and trapped air.

Each of the mass consistency ranges discussed above are important in the processing of pulp suspensions and in the papermaking process. For example, most paper-based products are formed from a suspension of 0.5 – 1% consistency, while medium to high consistency suspensions are used for bleaching and thickening. In papermaking, the finished product typically has a consistency of 90 – 95%, depending on the manufacturing specification and relative humidity. Ensuring that a suspension is of the desired consistency for a given process is of utmost importance for efficient and cost-effective operation on an industrial scale.

1.1.1.2 Fibre contacts and crowding number

Pulp fibres have a large aspect ratio (40 – 100) which induces significant contact among fibres in translational and rotational motion, even at very low consistencies. As

suspension consistency increases, inter-fibre collisions increase from occasional, to frequent, to continuous. The number of fibre contacts influences suspension properties greatly. Several contact regimes have been described using a crowding number, N , which is defined as the number of fibres in a spherical volume swept out by the length of an average fibre in the suspension [1]. The crowding number can be described in terms of mass consistency as follows:

$$N \simeq 5C_m \frac{(LW)^2}{\omega} \quad 1.2$$

where LW is length-weighted average fibre length [mm] and ω is fibre coarseness [mass per unit length of fibre, kg/mm]. N is a dimensionless quantity since it denotes the number of fibres within a specified volume, accordingly the units of the constant are kg/mm^3 [2].

Mason [3] suggested $N = 1$ as a “critical concentration” at which fibres first begin to collide with one another during flow. A second “critical concentration”, corresponding to $N \simeq 60$, was identified by Soszynski and Kerekes [4] and Kerekes and Schell [2], describing the crowding number at which fibres have approximately three points of contact with one another. The latter critical condition is of significance because three contact points are sufficient to restrain fibres in translation and rotation. Consequently, upon cessation of flow, fibres become interlocked and bent in a complex structure, imparting mechanical strength to the network through normal and frictional forces.

In later work, Martinez et al. [5] identified $N = 16$ as another “critical concentration”, calling this the “gel crowding number”. Below this value the suspension

behaves essentially as dilute, while above this value (but still below $N = 60$) fibres are in forced contact with one another, yet not completely restrained.

1.1.1.3 Forces on fibres and flocculation

Apart from frictional forces, there are several other forces that may contribute to overall fibre network strength. Kerekes et al. [1] identified some of these factors as forces imposed by the addition of chemical flocculants, hooking forces due to bent fibres, and surface tension forces due to significant air content.

Thus far, we have considered pulp fibre suspensions as homogeneous with regards to dispersion of fibres, however, in practice this is rarely the case. Below the rigidity threshold, fibres naturally translate and rotate relative to one another creating local mass concentrations known as flocs. Depending on flow conditions and fibre properties, the size and mechanical strength of flocs can vary significantly. For example, Kerekes [6] found that most flocs form in areas of decaying turbulence, such as immediately following a pump or mixer. Also, using a simulation method, Schmid et al. [7] found that curled fibres flocculated at $N < 1.5$ while straight, stiff fibres remained uniformly dispersed even at $N = 50$.

Flocs have a larger mass concentration than the suspension average, and thus also possess more strength than the suspension average. This results in flocculated suspensions being non-uniform in mass and strength, increasing the complexity of rheological (flow) analysis significantly.

1.1.2 Yield Stress

In the field of rheology, yield stress is defined as the shear stress required to cause a fluid to adopt continuous strain under a constant stress. More generally, the yield stress of a material is simply the pressure necessary to cause it to flow. A Newtonian fluid, water for example, does not have a significant yield stress, therefore any non-zero applied shear stress will result in shear flow. In the case of a Bingham plastic, which is a type of non-Newtonian fluid, the yield stress of the material must first be exceeded before shear flow will occur. In both cases, once shear flow begins, the ratio of shear stress to shear rate (i.e. the slope of a stress-strain curve) corresponds to the viscosity of the material.

Certain non-Newtonian fluids, known as Bingham pseudoplastics, possess a yield stress but do not exhibit a constant viscosity, instead, as shear rate increases, the slope of the stress-strain curve gradually decreases (i.e. viscosity is dependent upon shear rate). Another term used to describe this behaviour is “shear thinning”, which is used because the fluid becomes less viscous, or “thinner” as shear rate increases. Fibrous suspensions generally fall into this category of fluid.

There are various definitions of yield stress, as well as various means of measuring the property, consequently “apparent yield stress” is used to denote a yield stress value obtained via measurement.

1.1.2.1 Yield stress measurement techniques

Fibre suspensions exhibit flow characteristics of a Bingham pseudoplastic and consequently, at the onset of shear flow (shear rate > 0), viscosity immediately begins to decrease. Instantaneous viscosity can be plotted as a function of shear stress and the data

can be used to graphically determine the yield stress of the fibre suspension as the shear stress value at which the instantaneous viscosity begins to decrease [8, 9].

The yield stress of a fluid can also be measured using a torque versus time response. This method uses vaned rotors to apply a torque to the fibre suspension over time. The measured maximum torque is converted to the corresponding yield stress value. The rationale of this method is similar to that of the previous method, in that, at the point when the yield stress is exceeded, the viscosity of the suspension will begin to decrease. Accordingly, immediately before the decrease in viscosity, a maximum torque will be reached, which is then related to the apparent yield stress [10, 11].

Rheometry refers to the experimental techniques used in the study of rheological properties of fluids. Typically, a rheometer is used to monitor flow and deformation characteristics as a stress is applied to a fluid. A rheometer, rather than a viscometer, is used when the material being studied does not exhibit a single, constant viscosity. However, due to the previously mentioned complexities involved in measuring rheological properties of pulp suspensions, modified rheometers are used in practice as an alternative to a conventional device. Although beyond the scope of this thesis, several important modifications have been developed that can simplify and improve yield stress measurement [12, 13, 14, 15, 16, 17].

1.1.2.2 Apparent yield stress findings

All the work in this area demonstrated similar results: apparent yield stress depends on suspension consistency raised to a power. At relatively low consistency, for example 0.5 – 1.0%, the relationship takes the form:

$$\sigma_y = a(C_m - C_s)^b \quad 1.3$$

where σ_y is the apparent yield stress [Pa], a [Pa] and b are constants, C_m is the consistency of the suspension, and C_s is the “sediment” concentration. The sediment concentration, which is also a constant, is subtracted from the suspension concentration because the results indicate that consistencies below this threshold do not contribute to the overall mechanical strength of the fibre network [18]. Later, Martinez et al. [5] defined apparent yield stress in terms of crowding number and developed a similar expression:

$$\sigma_y = a(N - N_G)^b \quad 1.4$$

The only difference here is that N is the crowding number of the suspension and $N_G = 16$ is the gel crowding number, or “connectivity threshold” as described earlier.

When the consistency of a suspension is 3% or higher, a simpler expression is used which negates the “sediment consistency” or “connectivity threshold”.

$$\sigma_y = aC_m^b \quad 1.5$$

Many studies have used this expression to model apparent yield stress as a function of consistency, the results of which were summarized by Kerekes et al. [1]. Values of a vary from 1.8 – 24.5, while values of b vary from 1.69 – 3.02. There are several factors that may have contributed to these variations, such as differing measurement techniques and yield stress definitions. Also, many key variables that are now known to contribute to apparent yield stress differences were either not measured or not recorded. For

example, it is now understood that longer fibres result in a suspension having a greater apparent yield stress [15].

To analyze the data from the various studies in a meaningful way, Bennington et al. [10] defined a relative apparent yield stress, which is the apparent yield stress for a given test method divided by the average apparent yield stress of all the tests done using the same test method under similar experimental conditions. Using this method, data that was obtained under similar experimental conditions could be analyzed via a Gaussian distribution. The coefficient of variation for apparent yield stress of pulp fibre suspensions was 20%.

1.1.3 Fluidization of Pulp Suspensions

Fluidization is achieved when a sufficiently large stress is applied to a suspension causing it to adopt fluid-like characteristics, exhibiting relative motion between fluid elements. In the case of pulp suspensions, this is typically only possible under turbulent conditions, therefore turbulence and fluidization are often used interchangeably.

The stress required to induce fluidization has been studied extensively, mainly because transportation of a fluidized suspension can be achieved using a conventional centrifugal pump, even in the medium consistency range. On the other hand, a non-fluidized suspension, which has solid-like properties, would require a displacement pump to be transported.

One of the more interesting findings was that fluidization could take place at two levels: floc-level, and fibre-level, due to the large difference in stress required to achieve

each fluidization state [6, 14, 19]. Floc-level fluidization induces relative motion between individual floc particles and is typically sufficient for processes in which the suspension is pumped. Fibre-level fluidization, in which individual fibres move relative to one another, requires significantly more stress to be achieved. This level of fluidization is necessary for certain applications, such as in rapid, uniform mixing of chemicals throughout pulp.

Fluidization of pulp suspensions has been difficult to quantify due to a lack of direct measuring techniques. However, indirect methods have been developed to address this issue; for example, Bennington et al. [14] determined power dissipation, ε_f , per unit volume [W/m^3] as a function of mass consistency, ($1 < C_m < 12\%$), and equipment size.

$$\varepsilon_f = 4.5 \times 10^4 C_m^{2.5} \left(\frac{D_T}{D_R} \right)^{-2.3} \quad 1.4$$

Here D_T is the outer housing diameter and D_R is the rotor diameter of the impeller in the vessel. Using imaging techniques, fibre-level fluidization was observed at the rotor tips, while floc-level fluidization was observed away from the impeller, where power dissipation measurements were taken. The power dissipation at the rotor tips, required for fibre-level fluidization, was obtained by extrapolating the data to zero gap size (i.e. $D_R = D_T$). The results showed that the power dissipation required for fibre-level fluidization is approximately an order of magnitude greater than for floc-level fluidization. Numerous other studies have investigated the fluidization of pulp suspensions; however, the results have considerable scatter, most likely due to differences in measurement techniques.

1.1.4 Pulp Suspension Pipe Flow

Pipe flow is arguably the most important and prevalent type of flow used in transporting and processing pulp fibre suspensions on an industrial scale. Consequently, many workers have studied pipe flow properties of pulp suspensions as a function of process parameters, most notably, consistency and velocity.

In a key early study, Robertson and Mason [20] identified three distinct flow regimes for low consistency suspensions (0 – 8%), with the inter-regime transitions occurring as flow velocity changes. Since then, several other studies have revealed the same three flow regimes, which are illustrated in Figure 1.1. [21]. A plot of pipe friction loss, h_L , as a function of flow velocity, V , produces an “S” shaped curve which is shown in Figure 1.2. [21]. Note that the three regions illustrated in Figure 1.2. do not represent the three flow regimes, rather they are used as discrete intervals for sizing an appropriate pump based on the flow velocity required.

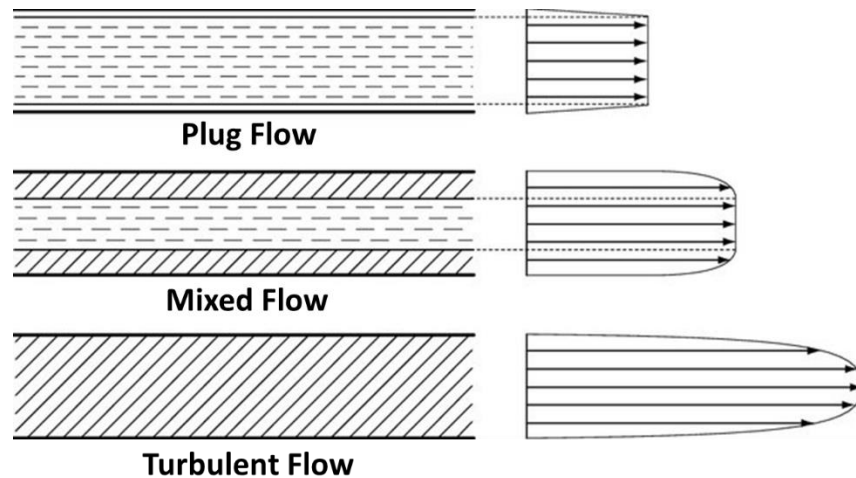


Figure 1.1. Flow regimes of pulp suspensions.

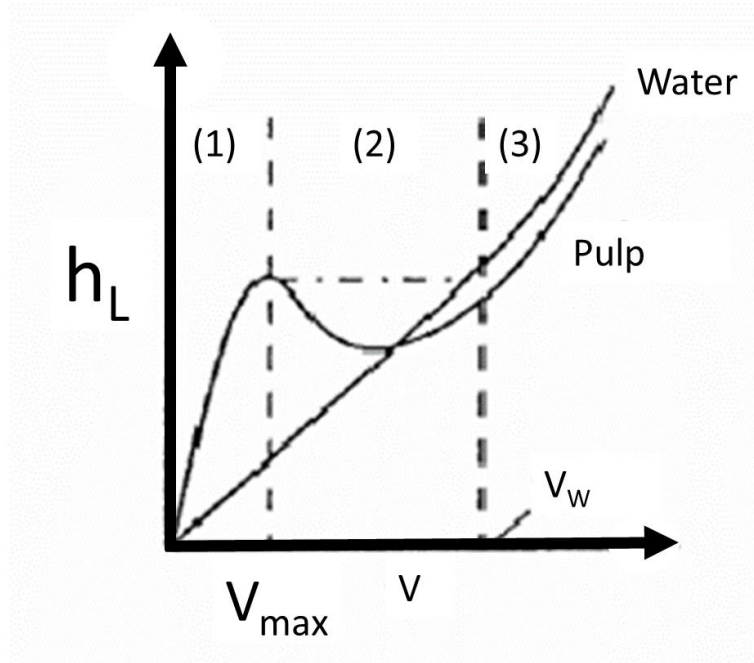


Figure 1.2. Pipe friction loss as a function of flow velocity.

At low velocity, “plug flow” occurs in which neither floc nor fibre-level fluidization takes place and the suspension flows essentially as a solid mass, with small flocs visibly “rolling” along the pipe walls. As flow velocity increases, shear at the pipe wall also increases, resulting in a clear water annulus forming between the pipe wall and the pulp plug (this occurs at the local maxima on the friction loss axis, denoted V_{max}). As velocity further increases, the size of this annulus increases at a greater rate than the velocity itself, causing an overall decrease in wall shear and decrease in friction loss (between V_{max} and the minimum preceding it). As velocity continues to increase, the annulus turns turbulent, deteriorating the exterior edges of the plug and mixing fibres into the annulus, marking the beginning of the “mixed flow” regime (local minima of the curve). With increasing velocity, shear also increases, resulting in an increase in the size of the turbulent annulus and a decrease in the size of the plug core. In this region, there

is a point at which the friction loss of the pulp suspension becomes less than that of water at the same flow velocity. This phenomenon is known as “drag reduction” and low consistency pulp suspensions were one of the first fluids known to exhibit this property. Eventually, as velocity continues to increase, the plug core is destroyed, and turbulence is achieved across the entire pipe diameter, marking the beginning of the third regime: “turbulent flow”.

For medium and higher consistency suspensions, these flow regimes do not apply, rather the suspension is in “plug flow” under almost all conditions due to the large amount of shear required to fluidize a suspension of this consistency. Additionally, suspensions in this consistency range will possess significant air content, making the suspension compressible. When compressed, the suspension will exert pressure on the pipe walls, leading to increased friction loss [22].

Various studies have modeled friction loss of pulp suspensions as a function of flow velocity [23, 24]. However, due to the previously discussed complications of pulp suspension flow properties, these models have been largely unsuccessful and of little practical use. Thus, empirical procedures are typically used in industry to estimate friction loss in pipe flow, for example Tappi Press TIP 0410-14 details a method which has been widely accepted as an industry standard [25].

1.1.5 Cellulose Dissolution

1.1.5.1 Polymer dissolution

The dissolution of polymers plays a key role in many applications, such as microlithography [26], controlled drug delivery [27], and biological tissue regeneration

[28], to name only a few. Understanding the dissolution mechanism, as well as the factors affecting dissolution, is a critical step in the design and optimization of polymer dissolution processes and allows for the selection of an appropriate solvent based on the specific application.

Polymers can undergo a so-called “glass-liquid transition” as temperature is increased, in which the material shifts from a hard and relatively brittle “glassy” state into a viscous or rubbery state. The glass transition temperature or T_g for dry cellulose fibres has been reported by many workers to be in the range 220 – 250 °C, which is well above the temperature at which cellulose begins to decompose [29]. Since decomposition is undesirable and the relevant pulping processes take place well below this temperature, dissolution will only be considered for polymers in their glassy state.

In early work, Ueberreiter studied the surface layers that are formed when a compatible solvent dissolves a glassy polymer, summarizing the results as shown in Figure 1.3. [30]. The first layer adjacent to the pure polymer surface is the infiltration layer. Here solvent molecules diffuse through holes and channels of molecular dimension present on the polymer surface, without creating any new holes or channels. Next is the solid swollen layer, here the polymer-solvent system is still in the solid state, however the polymer structure swells as it interacts with the solvent. The gel layer follows, consisting of swollen polymeric material in a gel-like state, followed by the liquid layer, composed of solvent molecules and the dissolved polymer. The final layer is simply the pure solvent.

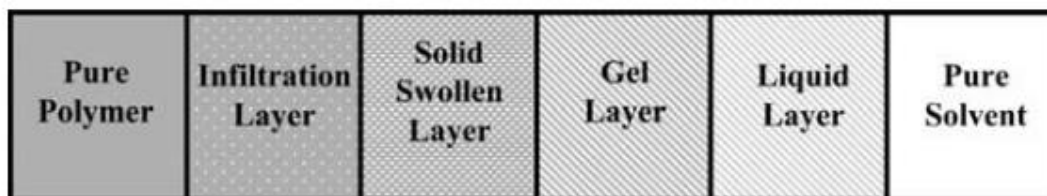


Figure 1.3. Schematic diagram of the surface layers formed during polymer dissolution.

There are several factors that have been shown to affect polymeric dissolution, for example: molecular weight, polydispersity, chemical structure, conformation, composition, chemical additives, and process conditions, among others. [31].

1.1.5.2 Cellulose dissolution in NaOH-water systems

It was in the mid 19th century that English scientist John Mercer discovered and patented mercerization, a process in which native cellulose fibres are treated by concentrated sodium hydroxide [32]. After immersion and washing, the treated fibres have improved properties such as increased lustre and smoothness, as well as better dye intake and improved mechanical properties. Mercerization itself is not a dissolution process, rather it results in a change in morphology and crystalline structure which occurs due to the highly-swollen state of the fibres and the formation of various alkali-cellulose complexes. The ease with which cellulose is mercerized depends on the degree of crystallinity, with low crystallinity fibres being mercerized more readily than highly crystalline ones [33].

There are conflicting views in the scientific community with regards to the mechanism through which mercerization proceeds, however, an important detail that

many authors agree on is that sodium ions disrupt the intermolecular hydrogen bonding network of cellulose, which is a necessary step in achieving the morphological changes that mercerization induces.

One of the more peculiar morphological changes that occurs when cellulose is placed in a swelling agent, such as NaOH, is the “ballooning” effect, a type of heterogeneous swelling that has been observed and described by many researchers from the late 19th and early 20th century [34, 35, 36]. One explanation for this phenomenon is that the swelling of the fibres of the secondary cell wall causes the primary wall to expand and tear. The secondary wall fibres further expand, penetrating through the tears of the primary wall which rolls up in such a way that “collars, rings, or spirals” form, restricting the uniform expansion of the fibre and thus inducing ballooning [37]. The ballooning effect is not limited to NaOH treatment, rather, ballooning will always occur before true dissolution if the solvent system is appropriate for cellulose dissolution.

The treatment of cellulose with sodium hydroxide has certain worthwhile applications, most notably cellulose activation. However, the dissolution of cellulose in this type of system is limited and can only be achieved in a narrow range of concentrations and temperatures. Sobue et al. [38] established the phase diagram of the cellulose-sodium hydroxide-water system, as shown in Figure 1.4. The various “Na-Cell.” regions of the phase diagram correspond to the different sodium-cellulose complexes that exist at a specific NaOH concentration and temperature. The dissolution range is from 7 to 10 wt.% NaOH and -5 to +1°C, thus dissolution of cellulose in sodium hydroxide has little industrial application since most pulp and paper processing takes place well above this temperature range (e.g. 60 – 80°C).

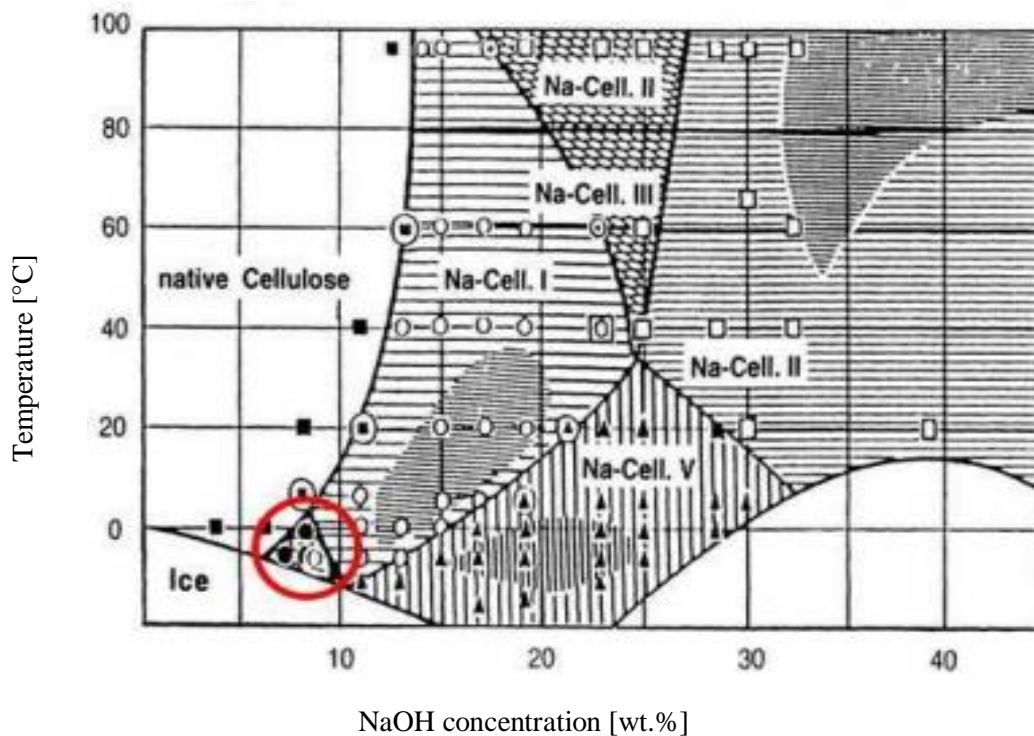


Figure 1.4. Phase diagram of the cellulose-sodium hydroxide-water system. The triangle encircled in red is the cellulose dissolution zone.

1.1.5.3 Cellulose dissolution in aqueous complexing agents

In 1857, Swiss Chemist Matthias Eduard Schweizer found that cotton could be dissolved in a solution of copper salts and ammonia and then regenerated in a coagulating bath [39]. This discovery was the basis for the family of solvents that are used in the dissolution and regeneration of cellulose for the commercial production of artificial silk. Several alternatives to this basic complexing agent have since been discovered, with each one containing a transition metal and an amine or ammonium component. Among these are:

Cuoxen ($[\text{Cu}(\text{NH}_2(\text{CH}_2)_2\text{NH}_2)_2][\text{OH}]_2$)

Nioxam ($[\text{Ni}(\text{NH}_3)_6][\text{OH}]_2$)

Nitren ($[\text{Ni}(\text{NH}_2\text{CH}_2\text{CH}_2)_3\text{N}][\text{OH}]_2$)

Pden ($[\text{Pd}(\text{NH}_2(\text{CH}_2)_2\text{NH}_2)][\text{OH}]_2$)

The dissolution of cellulose in Pden solution was investigated in detail by Kluefers et al. [40]. They found that this type of metal complex dissolves cellulose by deprotonating and coordinatively binding the hydroxyl groups of adjacent carbons centers, as illustrated in Figure 1.5.

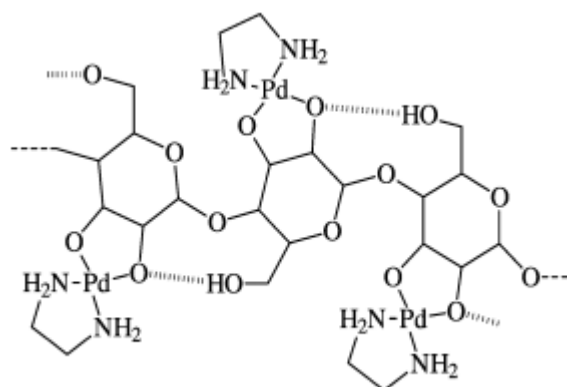


Figure 1.5. The proposed structure for dissolved cellulose in an aqueous solution of Pden.

In recent work, Arnoul-Jarriault et al. [41] investigated the swelling and dissolution of various dissolving pulps in Cuoxen, also known as cupriethylenediamine (CED) using a MorFi Analyser, which can measure width variations of thousands of fibres in a short amount of time. They found that an increase in the concentration of CED resulted in increased dissolution for CED concentrations from 0.10 M to 0.25 M.

When the pulp fibres were treated with the 0.10 M CED solution, no dissolution occurred. On the other hand, the 0.25 M treatment caused very strong swelling followed by complete fibre dissolution in under one minute. It was shown that swelling and dissolution also depend on the crystallinity and hemicellulose content of the fibres, where greater crystallinity and greater hemicellulose content both reduce dissolution. Surprisingly, dissolution did not depend on fibre origin (e.g. Kraft pulp, pre-hydrolysis Kraft pulp, sulfite pulp etc.) or degree of polymerization (DP). Figure 1.6 shows ballooning of a fibre in 0.20 M CED solution.



Figure 1.6. Intensive ballooning followed by total dissolution in 0.20 M CED solution.

1.1.5.4 **Other cellulose solvents**

Although not of interest for this thesis, there are several other classes of cellulose solvents that have been discovered and investigated. These include but are not limited

to: derivatizing solvents, NaOH/urea-based solvents, and molten organic salts (ionic liquids).

1.1.6 Inter-Fibre Frictional Forces

At high consistency, fibres are in forced contact with one another and consequently become mechanically entangled and develop various network structures, restricting their ability to rotate and translate freely. Under these conditions, inter-fibre contact area is increased and thus fibre friction (static friction especially) has a strong effect on network strength. Indeed, particle-level simulations [42, 43] have shown that static friction is essential to obtain elastic interlocking of fibres. Furthermore, Andersson et al. [44] measured the coefficient of friction between wet fibre surfaces and found that $\mu = 0.6 - 0.8$. In addition to this result, they also noticed an “adhesive force”, obtained by extrapolating the friction data to zero normal force. They suggest that it could be due to an electrochemical effect since it increased with increasing ionic strength [44].

1.1.6.1 Polymer addition to reduce friction

Many water-soluble polymers (WSPs) have been used as rheological modifiers for biomass-based suspensions. Samaniuk et al. [45] tested carboxymethyl cellulose (CMC), polyethylene oxide (PEO), and polyacrylamide (PAM) and found that the yield stress of concentrated biomass could be reduced by as much as 60 – 80% with a polymer dosage of only 1 – 2 wt.%. The degree to which the yield stress could be decreased was shown to depend on polymer molecular weight as well as degree of substitution. Furthermore, Stiernstedt et al. [46] showed that xyloglucan adsorbs strongly onto cellulose, resulting in increased repulsion between approaching cellulose surfaces, consequently reducing inter-fibre friction.

The mechanism through which WSPs act to reduce inter-fibre friction, and therefore yield stress, remains largely unconfirmed. Zauscher and Klingenberg [47] employed colloidal probe microscopy to show that CMC and cationic-PAM (C-PAM) could reduce the coefficient of sliding friction between model cellulose surfaces. They propose a mechanism in which polymer adsorption smoothens the fibre surface, thus allowing fibres to slide past one another with less resistance. Mosse et al. [48] investigated the effect of C-PAM treatment on the yield stress of dilute hardwood pulp suspensions (2.5 wt.%). Charge density of the polymer proved to have the strongest effect on yield stress, while variations in molecular weight had a smaller effect. Several possible mechanisms are proposed to explain how C-PAM can modify the interactions between cellulose surfaces. Of these, electrostatic charge neutralization and electrostatic patch formation are thought to dominate, while polymer bridging and steric repulsion also influence the interaction, albeit to a smaller extent.

1.1.7 Fibre-Based Pipeline Plugging

In pulp and paper operations, pulp fibre-based plugs of significant strength can form within pipelines and equipment, consequently restricting flow. Downstream processes are likely to be affected, thus shutting down production may be necessary. In some cases, pressurized steam or air can be used to remove the blockage, however, this can be detrimental to process equipment and is also a safety hazard. Alternatively, operations may be shut down temporarily to allow for the plug to be removed manually. Similarly, this is not an attractive option due to operational downtime and increased labour costs.

The strength of a fibre network has been shown to depend on the network consistency, fibre aspect ratio, fibre stiffness, and inter-fibre frictional forces [49, 50, 10]. Additionally, during pressure-driven de-plugging efforts, the consistency (or solids content) of the fibre network will increase due to compression and dewatering effects. Hewitt et al. [51] concluded that the rate at which consistency increases is dependent upon the applied pressure, fibre properties, and dewatering properties of the network.

1.2 Thesis Objectives

The overall objective of this work was to develop a safe and effective approach for the removal of fibre-based plugs from pipelines and equipment. Such an approach would be validated on a laboratory bench-scale to demonstrate its potential application in industrial operations. The specific objectives of this thesis can be summarized as follows:

- 1) To build an experimental apparatus that can be used for measuring the fibre network strength (i.e. break-up pressure) and to determine the effect of experimental conditions on the break-up pressure (Chapter 2).
- 2) To propose a chemical additive that can reduce the required pressure-head for plug removal and to understand its associated mechanism of action (Chapters 2 and 3).

2 Using Cupriethylenediamine (CED) Solution to Decrease Cellulose Fibre Network Strength for Removal of Pulp Fibre Plugs

2.1 Abstract

The pulp and paper industry is the largest industrial sector which converts wood-based materials into fibre-related products. Commonly, pulp fibre plugs occur within pipelines and equipment causing operational downtime requiring costly procedures for their removal. In this study, a simple bench-scale set-up was developed to measure the break-up pressure of pre-formed plugs to indicate the plug (fibre network) strength. The plug strength was tested by treatment with water and various concentrations of cupriethylenediamine (CED) solutions. The results showed that the break-up pressure has a power-law relationship with plug mass when plug dry-masses are between 3.0 – 5.0 g, and that the break-up pressure decreased with increasing center hole size (25 – 30 mm). Furthermore, cupriethylenediamine (CED) solutions of varying concentration were tested for their ability to decrease the plug strength. For CED solutions with a concentration of 0.15 M and 0.2 M the plug break-up pressure decreases significantly due to fibre dissolution.

2.2 Introduction

The flow of fibre suspensions is essential within flow delivery systems in the manufacturing of various bio-derived products [49], such as pulp & paper [52, 53], lignocellulosic biofuels [54, 55], plant tissue based foods [56, 57], and polymer composites [58]. The pulp and paper industry, which is the largest among these,

typically uses wood (e.g. pine, spruce, and eucalyptus), non-wood (e.g. wheat straw and bamboo), and recycled fibres as the raw material in producing pulp, paper, paperboard, and cellulose-based products.

In pulp and paper process streams, pulp-fibre related plugs and/or blockages can occur within pipelines and equipment. These plugs may occur rapidly, thereby affecting several downstream processes simultaneously and ultimately causing unexpected production shut-downs. One method that can be used to remove a blockage is to apply a pressure head using pressurized steam or air; however, this approach can be detrimental to operating equipment and may pose a safety hazard to nearby workers. This process results in increased labor costs and operational downtime. Thus, it is necessary to develop a safe and efficient method for removing pulp fibre plugs (de-plugging).

De-plugging of pulp fibre plugs is a complex phenomenon which depends mainly on the strength of the fibre network that is formed. When attempting to remove a plug with an applied pressure head, the plug first undergoes compression, then as the pressure exceeds the strength of the fibre network, collapsing occurs. The strength of a fibre network has been reported to depend on the consistency of the plug, fibre aspect ratio, fibre stiffness (flexibility) and inter-fibre friction [49, 10, 50]. Kerekes et al. [42, 43], introduced the concept of a crowding factor, which describes the frequency of fibre-fibre collisions. They demonstrated that when the crowding factor of a fibre suspension is approximately 60, each fibre makes three contact points with other fibres. Furthermore, they demonstrated that under these conditions fibres are in continuous contact with each other and are prone to be interlocked in bent configurations. Bennington et al. [10] developed a theoretical model describing fibre network strength

based on the interlocking of elastically bent fibres. In this elastic-interlocking model, the yield stress is an indication of the fibre network strength and depends on suspension consistency, fibre aspect ratio, and fibre Young's modulus. Lastly, particle-level simulations [42, 43] show that inter-fibre frictional forces, especially static friction, play a key role for inducing fibre flocculation.

In the context of this work, the yield stress of a fibrous suspension is defined as the minimum stress necessary to disrupt the network and commence flow of the suspension [17]. It is often used to describe fibre network strength and is a vital rheological parameter of pulp fibre suspensions [49]. However, the measurement of yield stress is difficult for two main reasons: 1) fibres and flocs are prone to slip along the wall of their measurement container; and 2) at high consistency, floc sizes are large (~25 mm) relative to the particle size in a conventional particle suspension (~1 mm) [59]. For suspensions at low and medium consistencies (<20%), devices for measuring yield stress are classified mainly into two groups: vaned-geometry devices and modified parallel plate devices [60]. At high consistencies (20-40%), torque rheometers [61, 62] and auger-based rheometers [55] are typically employed to measure yield stress.

Due to plug compression during pressure driven de-plugging processes, the pulp consistency, or solids content, increases as the plug is compressed. Moreover, the rate at which the consistency increases depends on the pressure, fibre properties, and dewatering properties of the fibre plug [51]. In this study, one objective was to develop a laboratory-scale set-up that could simulate a pressure-driven plug breaking process within a pipeline.

Wood fibres are natural composite structures consisting mainly of cellulose, hemicellulose, lignin, and extractives, with the relative amount of each component depending on many factors, including pulping method. Cellulose dissolution, or partial dissolution, can be an effective approach to decrease the fibre network strength. Cellulose solvents can be classified into two types: aqueous and non-aqueous solvents. Aqueous solvents include NaOH, NaOH/urea [63], phosphoric acid [64], transition metal complexes [65], and others, while non-aqueous solvents include dimethylacetamide/LiCl [66], N-methylmorpholine-N-oxide (NMMO) [67], ionic liquids [68], and others. For convenience within mill operations, chemical solvents should be mixed in process water for their application; therefore, non-aqueous solvents are not suitable. Some of these solvents have obvious drawbacks, for example, phosphoric acid can induce pipeline and equipment corrosion; and NaOH or NaOH/urea-based systems require low temperatures ($<0^{\circ}\text{C}$) for fibre dissolution, posing complications in their use [69].

A solution of Cupriethylenediamine (CED or CUEN) in water is capable of cellulose dissolution, and CED itself falls within the category of transition metal complexes. Moreover, CED possesses favorable properties, such that even at dilute concentrations and room temperature, cellulose dissolution occurs. This can be an attractive solution for mill operations. Another objective of the present study was to use CED solution for decreasing the fibre network strength.

The present study includes a performance assessment of the set-up, in which the effects of plug mass, center hole size, and input pressure rate on the break-up pressure were investigated. The set-up was used to assess the use of CED solution in decreasing

the pressure head required to break the fibre plug. Additionally, the effect of CED concentration on the break-up pressure was investigated and an analysis of the mechanisms through which CED acts in decreasing the break-up pressure is included.

2.3 Materials and Methods

2.3.1 Materials

A Canadian-produced northern bleached softwood Kraft (NBSK) pulp was used in this study. A CED commercial solution of 1.0 M was purchased from Sigma-Aldrich Co., Canada. Diluted solutions of CED were prepared by mixing the commercial solution with tap water.

2.3.2 Experimental Set-up

2.3.2.1 Set-up for measuring plug break-up pressure

The experimental set-up for measuring the plug break-up pressure is shown below in Figures 2.1 and 2.2. The apparatus consisted of a 2-inch diameter plastic column, a pressure transducer (Omega Engineering, PX209-100G5V), an air compressor, a diaphragm pump (Shurflo, 8030-863-239BX), a collection tank, a storage tank, and a fluid level control system. The column was divided into two sections joined by a union. The top section was equipped with two injection ports and topped with a cap, where the top port was used to input air for the applied pressure head, and the bottom port to input the operating fluid. The pressure transducer was installed in-line prior to the top injection port to monitor the air input pressure. The bottom section of the test column had a porous bottom plate containing a center hole through which a pre-formed plug would flow through upon breaking. The fluid level control system consisted

of two conductivity probes, two electromagnetic valves, a data acquisition (DAQ) board (USB-6215, National Instrument Co.), and a computer. The fluid level was controlled via the change in conductivity between the two probes located below the fluid injection port. When both probes were submersed in the operating fluid, the corresponding conductivity caused the first electromagnetic valve to open and the second to close, recycling the fluid back to the storage tank. As the fluid level decreased, exposing the top probe to air, the decrease in conductivity prompted the first electromagnetic valve to close and the second to open. The fluid then filled the test column until the top probe was submersed once again, and the cycle repeated for the duration of the experiment.

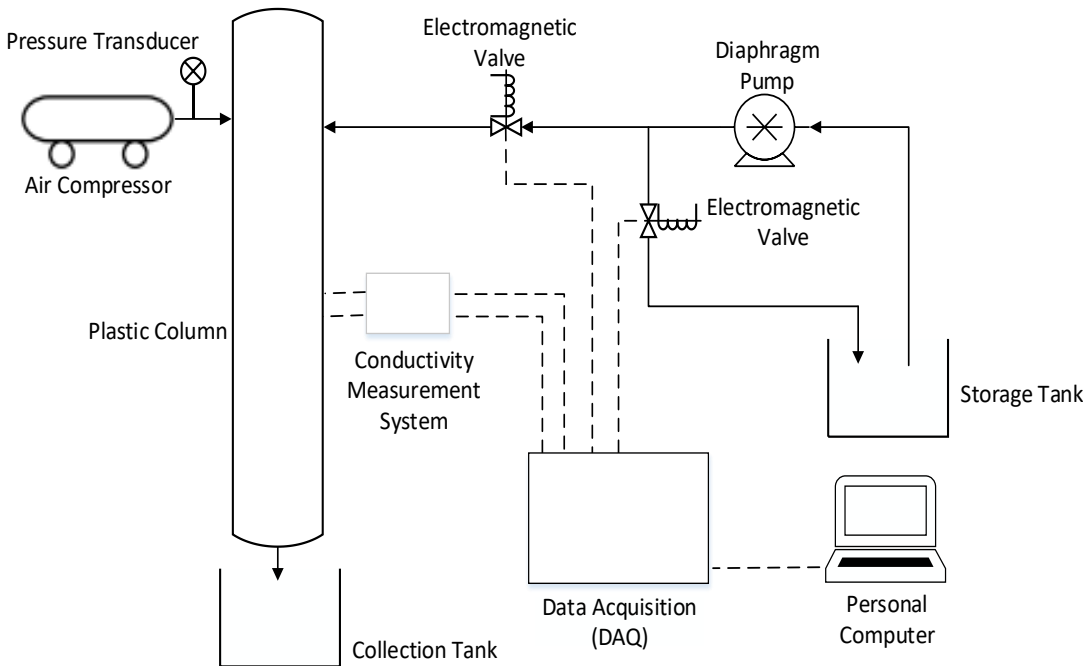


Figure 2.1. Schematic diagram of the experimental set-up for measuring the plug break-up pressure.

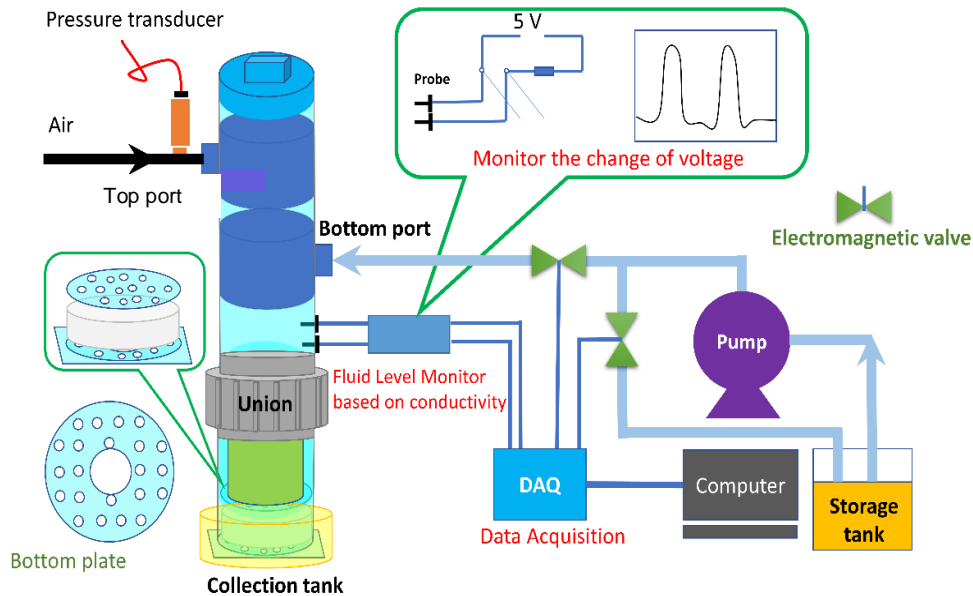


Figure 2.2. Cartoon diagram of experimental set-up for measuring the plug break-up pressure.

Two design principles were implemented for measuring the break-up pressure using the experimental set-up. The first principle was that the pre-formed plug would be broken by applying a sufficiently large pressure head to it. This was accomplished by inputting compressed air through the top injection port, thereby pressurizing the operating fluid and thus the plug itself. The second principle was to ensure that the top and bottom of the plug maintained continuous contact with the operating fluid, simulating conditions within pipelines. This was accomplished by maintaining the fluid

level within the column at approximately 20 cm above the plug while submersing the bottom of the plug in the fluid within the collection tank.

2.3.2.2 Set-up for plug formation

Prior to performing de-plugging experiments, the plug was manually formed from a dilute fibre suspension according to the following procedure. A stainless-steel mesh (250 mesh) and a porous plate were positioned under the bottom plate of the test column's bottom section, and the three parts were held together by two clamps. The diluted fibre suspension (~0.8 wt.%) was then poured through the mesh, retaining the fibres as a wet plug within the column, and subsequently drained of excess water by gravity. To keep the initial consistency of the plug constant, a second porous plate (of equal diameter to the column's inner diameter) was placed on top of the formed plug and manually pressed down to a specified thickness that corresponded to a plug consistency of approximately 15 wt.%. Now containing the formed plug, the bottom section of the test column was then coupled with the top section using the union as shown in Figure 2.2. The plug was then soaked with the operating fluid (tap water or CED solution) by maintaining the fluid level at a constant height above the plug for a duration of 10 minutes, where the total volume of the fluid that passed through the plug was at least 8 times the initial volume of the plug. While soaking, the bottom porous plate, mesh, and clamps were held together to minimize mass loss of non-dissolved fibres during soaking. After soaking, the clamps, porous plate, and mesh were removed, and the pressure was gradually increased using compressed air while maintaining a constant fluid level as described previously. When the pressure exceeded the strength of the plug, the plug collapsed through the center hole of the bottom plate, designating the break-up pressure.

All measurements were made in quintuplicate and error bars presented in figures represent their standard deviation.

2.4 Analytical Methods

2.4.1 Water Retention Value

The water retention value (WRV) of the pulp samples in this study was determined based on a centrifugation method [70], which employed a centrifuging force of 900 g for 30 min. The WRV was determined for pulp samples before and after treatment in the operating fluid to observe changes in water retention.

2.4.2 Mass Loss

The plug mass loss was calculated as the difference of the plug mass before and after treatment with the operating fluid. All samples were oven-dried overnight to determine their dry mass for the mass loss calculation.

2.4.3 Degree of Polymerization

The average degree of polymerization (DP) of the pulp samples was calculated from the pulp viscosity using equation 2.1 [71]. The pulp viscosity was measured using the capillary viscometer method as described by the TAPPI standard T230 [72].

$$DP^{0.905} = 0.75[954 \log_{10}(\eta) - 325] \quad 2.1$$

where η is the TAPPI viscosity [cp].

2.4.4 Fibre Properties

The fibre properties of the pulp samples were analyzed using a classic FQA (code LDA96, OpTest Equipment Inc.). The measured fibre properties include fibre

length, fines content, and fibre coarseness. For evaluating changes in fibre properties, the FQA analysis was performed for pulp samples before and after treatment with the operating fluid.

2.4.5 Microscopy Observation

Using a pipette, individual wet fibres of NBSK pulp were placed on a glass slide. A top plate was then placed on the glass slide, and pictures of the fibres were captured using an optical microscope (Leica DM4000 M, Leica Microsystem (Canada) Inc.). The top plate was then removed and the water surrounding the fibres was removed with an absorbent paper. Three to four drops of CED solution (0.1 or 0.2 M) were then placed onto the fibres. After 5 – 10 minutes, a new top plate was placed on the glass slide, and pictures of the CED treated NBSK fibres were captured.

2.5 Results and Discussion

2.5.1 Plug Break-up Pressure Measurement

As mentioned previously, as the pressure applied to the plug increases, the plug will compress accordingly. It was observed that when the applied pressure was low, a small displacement of the plug through the center hole of the bottom plate occurs. As the pressure approaches the plug break-up pressure, this displacement becomes more pronounced until collapse occurs. A typical pressure signal for determining the break-up pressure during de-plugging trials is shown below in Figure 2.3. The break-up pressure was estimated by the peak of the pressure signal as the plug broke through the center hole. All break-up pressure measurements were gauge pressures (i.e. psig rather than psia).

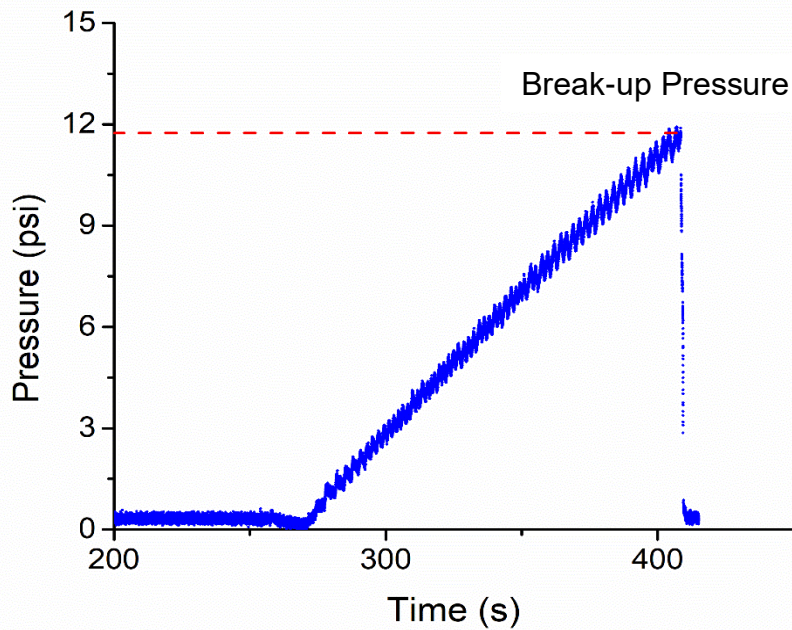


Figure 2.3. Typical pressure signal for determining the plug break-up pressure for the de-plugging trials.

2.5.2 Effect of Input Pressure Rate

The break-up pressure, P_b , is shown as a function of input pressure rate in Figure 2.4. The results indicate that P_b does not depend on input pressure rate when the rate is less than approximately 13.6 psi/min. Thus, all subsequent measurements were made at an input pressure rate of 8 – 12 psi/min.

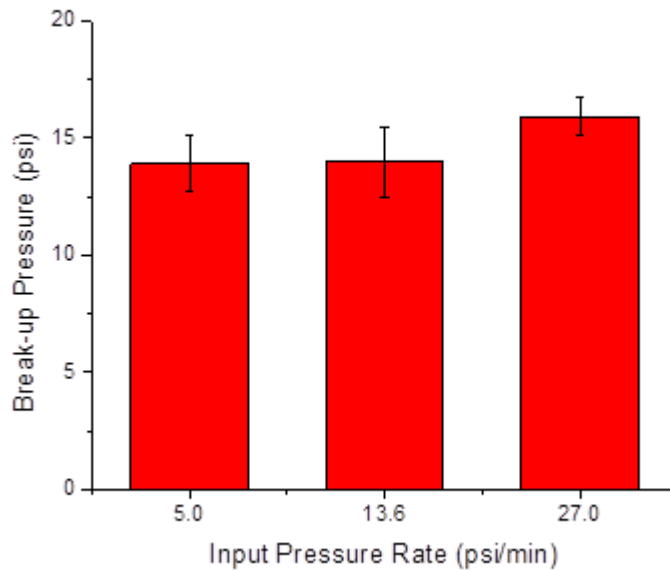


Figure 2.4. Effect of input pressure rate on break-up pressure.

2.5.3 Effect of Bottom Plate Center Hole Diameter and Plug Mass

Figure 2.5 shows the break-up pressure as a function of plug mass at varying center hole diameters. Two center hole sizes of 25 and 30 mm were evaluated, and for both, the break-up pressure increases rapidly with increasing plug mass (or initial pulp consistency of the plug), which is well represented by a power law expression with exponential values of 3.45 and 2.97, respectively. This power law dependency is similar to that which many researchers have demonstrated, where yield stress increases rapidly with increasing suspension consistency [17]. It was also observed that when the plug mass is held constant, the break-up pressure increases with decreasing center hole size. This result was expected due to there being a smaller flow channel for the plug to flow through upon collapse. As the plug mass increases, the difference in break-up pressure between the different center hole sizes also increases. From this observation, a center

hole size of 25 mm was selected to perform the de-plugging trials, as changes in pressure are more pronounced at this size, which is useful for comparing the different plug treatments.

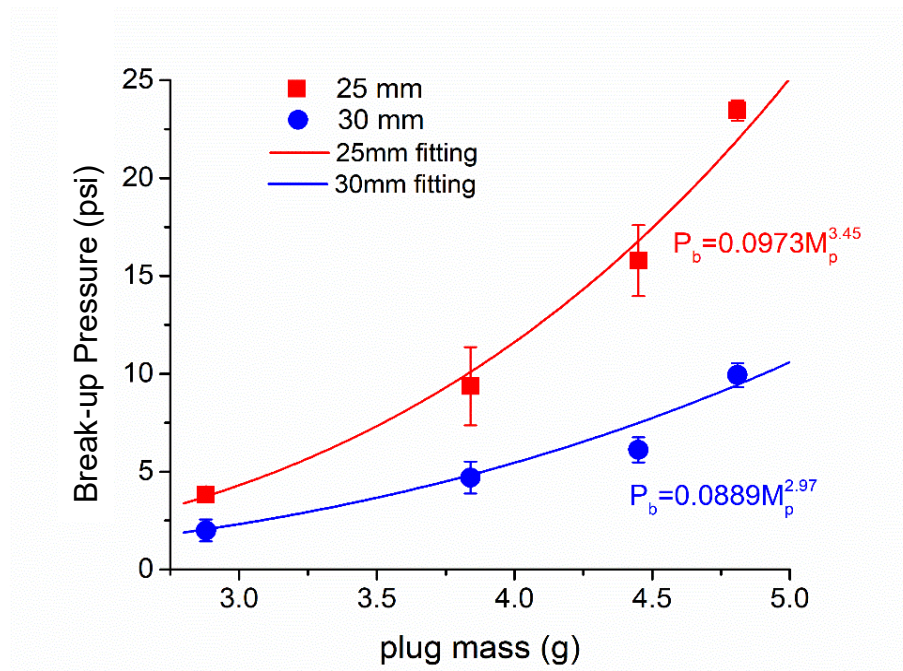


Figure 2.5. Break-up pressure as a function of plug mass at constant initial plug consistency for two different center hole diameters.

2.5.4 Effect of CED concentration

Figure 2.6. shows the effect of CED concentration on the break-up pressure for a plug mass of 3.85 g and a reaction (soaking) time of 10 minutes. After the reaction time had elapsed, the operating fluid was changed to tap water to reduce the usage of CED solution. When the CED concentration is below or equal to 0.1 M, the break-up pressure increases with increasing concentration, however, when the CED concentration is 0.15

or 0.2 M, the break-up pressure decreased significantly. These results imply that there is a critical concentration at which the break-up pressure begins to decrease.

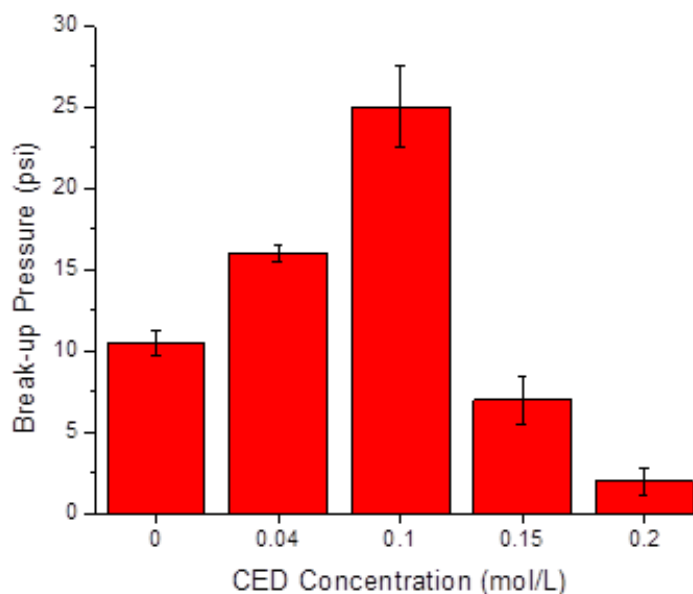


Figure 2.6. Effect of CED concentration on break-up pressure for a plug mass of 3.85 g and a 10-minute reaction time.

Table 2.1 lists the NBSK fibre properties before and after CED treatment at concentrations of 0.1 M and 0.2 M. After a reaction time of 10 minutes, the 0.1 M and 0.2 M CED treated fibres exhibit significant differences in their properties. As shown, the WRV increases with increasing CED concentration and for the 0.2 M CED treatment the WRV of the treated fibres is greater than twice that of the original fibres. Since an increase in WRV is indicative of fibre swelling, these results show that swelling takes place at a significantly greater rate for the 0.2 M CED treated fibres compared to the 0.1 M CED treated fibres.

Table 2.1. Change in fibre properties from various 10-minute CED treatments.

Parameter	Original fibre	0.1 M CED treated fibre	0.2 M CED treated fibre
WRV [g/g]	1.12±0.04	1.36±0.02	2.38±0.08
Mass loss [%]	1.6±1.3*	1.2±1.3	10.1±0.6
DP (-)	990±10	940±50	970±10
LN** [mm]	1.04±0.05	1.0±0.02	0.72±0.02
LW*** [mm]	2.16±0.03	2.07±0.03	1.90±0.02
LWW**** [mm]	2.65±0.01	2.58±0.03	2.46±0.03
Coarseness [mg/m]	0.175±0.01	0.195±0.017	0.248±0.019

* Control sample for mass loss of untreated fibres

** LN is numerical average length

***LW is length-weighted average length

****LWW is weight-weighted average length

From the results of mass loss, fibre length, and fibre coarseness, it is evident that for the 0.2 M CED treatment partial fibre dissolution occurs. When the fibres are soaked in the 0.1 M CED solution the mass loss after a 10-minute treatment is negligible when compared to a control sample of untreated NBSK fibres. However, the mass loss for the 0.2 M CED treated fibres was approximately 10.1% after 10 minutes. Furthermore, the fibre length changed slightly for the 0.1 M CED treatment, but for the 0.2 M CED treatment, the average length, length-weighted average length, and weight-weighted average length change from 0.85 mm, 2.05 mm and 2.62 mm to 0.72 mm, 1.90 mm, and 2.46 mm, respectively. The 0.2 M CED treatment results in an increase in fibre coarseness from 0.175 ± 0.004 mg/m to 0.248 ± 0.019 mg/m. Since coarseness is measured per unit length of fibre, the increase in coarseness is attributed to the decrease

in fibre length that was observed for the 0.2 M treatment. After treatment, the fibres were examined using optical microscopy and results similar to those demonstrated by Arnoul-Jarriault were observed [41]. The captured images are shown in Figure 2.7.



Figure 2.7. Optical microscopy images of original and CED-treated pulp fibres.

Cuissinat and Navard [37] summarized five modes to describe the behavior of cellulose fibres in a chemical solution. Two of these five modes were observed using optical microscopy in this study. The first, mode 3, is large fibre swelling observed as ballooning, followed by partial dissolution whilst maintaining the fibre's shape. The second, mode 4, is homogenous swelling where no dissolution of any part of the fibre occurs. The ballooning phenomena is characterized by swelling of the secondary fibre wall, which causes the primary wall to expand and burst [73]. This ultimately depends on the presence of the primary wall, as well as the solvent quality [74]. Cuissinat et al. [69, 75, 76] also observed fibre swelling and dissolution in various cellulose solvents. They concluded that the mechanisms of swelling and dissolution are universal, meaning that they do not depend on the fibre origin, but only on solvent quality.

For the 0.1 M CED treatment, only loosely-packed, amorphous regions of the fibres are penetrated with CED, while the highly ordered, crystalline regions are inaccessible. It is suspected that this is due to low rates of diffusion of the solvent into the fibre, which is driven by the concentration gradient between the bulk solution of CED and the CED penetrating the surface of the fibre. Therefore, the increase in break-up pressure can be attributed to two factors: 1) the stiffness of the treated fibres, which is related to their crystalline structure [77], changes negligibly; and 2) the swelling of the treated fibre, which results in an increase in the contact area and the number of contact points between fibres. At higher concentrations, i.e. 0.15 and 0.2 M, it is suspected that CED can access the crystalline regions of the fibres due to improved solvent diffusion into the fibre, resulting in partial dissolution of the secondary cell wall and thus the characteristic balloon formation. Once these ballooned regions reach their expansion limit, rupture occurs, thereby shortening the length of fibres by means of fragmentation. Therefore, the decrease in break-up pressure can also be attributed to two factors: 1) the stiffness of the treated fibres decreases due to partial fibre dissolution within crystalline regions; and 2) balloon rupturing and fibre dissolution, both of which decrease fibre length.

2.5.5 CED-Assisted De-Plugging Mechanism

In summary of the findings in Section 2.5.4, there are two key mechanisms that can take place when CED solution is used as a solvent to assist in plug removal: swelling and dissolution (see Figure 2.8). The swelling mechanism is dominant at low concentrations (0.04 and 0.1 M), where CED can only penetrate amorphous regions of the fibres, resulting in fibre swelling. Swelling increases the number of contact points

and the contact area among fibres, which can increase the friction or inter-locking force between fibres, resulting in an increase in the fibre network strength and thus the break-up pressure. The dissolution mechanism is dominant at higher concentration (0.15 and 0.2 M), where fibre swelling followed by partial fibre dissolution occurs. Though fibre swelling can increase the number of contact points and the contact area among fibres, the decrease in fibre stiffness and fibre length caused by fibre dissolution and balloon rupturing results in an overall decrease in fibre network strength, thus decreasing the break-up pressure.

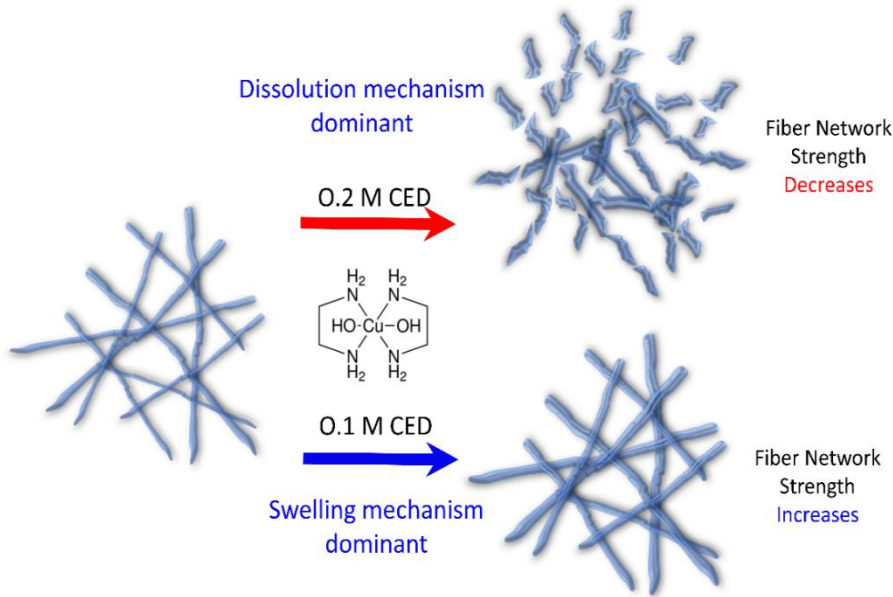


Figure 2.8. The mechanisms through which CED solution affects fibre network strength.

2.6 Conclusions

A laboratory-scale set-up that can indicate fibre network strength was developed to measure the break-up pressure of a wood pulp fibre plug system. Its key feature was to simulate a pipeline de-plugging process, which was accomplished using compressed air to apply a pressure head to break the plug. The main components of the experimental set-up included a test column, a pressure sensor, a fluid level control system, and an air compressor. The results showed that the break-up pressure has a power-law relationship with plug mass when the plug mass ranges from 3.0 – 5.0 g. Furthermore, the break-up pressure decreases with increasing center hole diameter (25 – 30 mm) in the bottom plate. Lastly, the effect of input pressure rate has a negligible impact on results when it is lower than 13.6 psi/min.

Cupriethylenediamine (CED) solution was used as a chemical solvent for assisting in the de-plugging of wood pulp fibre plugs. The results show that a CED concentration of 0.1 M increases the break-up pressure from 11 psi to 24 psi for a 10-minute reaction time. When the CED concentration is 0.2 M the break-up pressure decreases significantly from 11 psi to 2.0 psi for the same reaction time. The mechanisms through which CED functions are: 1) swelling at low CED concentration (0.04 and 0.1 M), which increases the contact points and the contact area among fibres, consequently increasing the fibre network strength; and 2) dissolution at high CED concentration (0.15 and 0.2 M), where fibres are susceptible to dissolution and shortening by fragmentation, resulting in an overall decrease in the fibre network strength.

3 Using Cationic Polyacrylamide (C-PAM) Solution to Decrease Cellulose Fibre Network Strength for Removal of Pulp Fibre Plugs

3.1 Abstract

The pulp & paper industry is the industrial sector in which biomass is converted to various fibre-derived products. A common issue experienced in pulp processing is the blockage of pipelines by strong plugs of compacted fibre networks, potentially resulting in time consuming and costly procedures being employed for their removal. In this study, the plug break-up pressure, measured using a laboratory-scale set-up, was used to represent the plug strength. Cationic polyacrylamide (C-PAM) solution was used for decreasing the pressure head required to break the plug. The results show that a low concentration of C-PAM solution can decrease the break-up pressure of softwood and hardwood-based plugs, and that the reduction in break-up pressure is mainly caused by the adsorption of C-PAM onto the pulp fibre surface. A 100 ppm C-PAM solution is sufficient for decreasing the break-up pressure when the reaction time is 30 minutes and the initial plug consistency is 15 wt.%. However, when the initial plug consistency is increased to 35 wt.%, applying the C-PAM solution under pressure is necessary for achieving a similar reduction in break-up pressure within a shorter reaction time of 5 minutes. Additionally, the proposed mechanism through which C-PAM assisted de-plugging functions is discussed.

3.2 Introduction

In a pulp fibre network of high consistency, each fibre has at least three points of contact with other fibres and is consequently restricted in rotation and translation. Therefore, due to the high contact surface area between interlocked fibres, inter-fibre friction becomes an important property in determining the yield stress and overall strength of a fibre network. Particle-level simulations [42, 43] have shown that inter-fibre frictional forces, especially static friction, play a key role in inducing fibre flocculation.

Charged polymers (polyelectrolytes) have lubricating properties and therefore can be used in reducing frictional forces. Raviv et al. [78] showed that charged polymer brushes, which are surface coatings consisting of charged polymers tethered to a surface, have excellent lubrication properties. They used a poly(methyl methacrylate)-block-poly(sodium sulphonated glycidyl methacrylate) copolymer brush and found that superior lubrication could be achieved, attributing the results to the characteristics of compressed, counterion-swollen brushes and the fluidity of the hydration layers surrounding the polymeric segments. Samaniuk et al. [45] investigated several water-soluble polymers (WSPs) for modifying the rheology of lignocellulosic biomass (20 – 25 wt.% solids) and found that the yield stress of the suspension could be decreased by 60 – 80% with a WSP addition of as little as 1 – 2 wt.%. Zauscher and Klingenberg [47] used colloidal probe microscopy to show that adsorbed carboxymethyl cellulose (CMC) and cationic polyacrylamide (C-PAM) can reduce the coefficient of sliding friction between model cellulose surfaces. The decrease in the coefficient of friction was attributed to polymer concentration in the suspending medium, as well as polymer molecular weight, shape,

and charge. They propose that the inter-fibre friction is reduced due to the adsorption of polymers onto fibre surfaces, thus masking surface asperities and allowing fibres to slide past one another with less resistance. Stiernstedt et al. [46] demonstrated that xyloglucan adsorption onto cellulose surfaces significantly reduces fibre friction, attributing the result to an increase in repulsion between the modified cellulose surfaces. Furthermore, Mosse et al. [48] investigated the effect of C-PAM on the interactions between cellulose fibres at low consistency (2 wt.%), and found that at high C-PAM concentrations (> 4 mg C-PAM/g cellulose) the suspension becomes positively charged overall, resulting in strong electrostatic repulsions between the polymer-coated fibres, thereby decreasing the yield stress of the suspension. These studies have shown that charged polymers can be effective for decreasing the inter-fibre friction and yield stress at low and medium consistencies (<20 wt.%); however, the consistency of a pulp fibre plug is typically significantly greater than this. Accordingly, it is of interest to investigate the use of cationic polymers for the removal of pulp fibre plugs.

C-PAM is traditionally used in the papermaking industry as a retention aid, where its function is to retain fine particles in the final paper product through polymer bridging and charged-patch formation mechanisms [79]. Thus, if C-PAM is employed for de-plugging purposes in a paper mill where C-PAM will also be used as a retention aid, the quality of the final paper product is unlikely to be compromised. In this study, different concentrations of C-PAM solution were investigated to determine their effectiveness in breaking pre-formed plugs prepared from bleached softwood or hardwood pulp. The effect of the initial pulp consistency of the plug, reaction time, and pre-pressure treatment were also investigated. Finally, the relationship between the

adsorption of C-PAM onto the pulp fibres and the plug break-up pressure was quantified.

3.3 Materials and Methods

3.3.1 Materials

Canadian-produced northern bleached softwood Kraft (NBSK) pulp and bleached hardwood Kraft (BHK) pulp, were used in this study. Percol[®] 175, a copolymer of acrylamide and an acrylic acid salt, with a molecular weight of $(5.0 \pm 1.0) \times 10^6$ g/mol and a charge number density of 1.1 meq/g [47] was purchased from BASF Corporation and was used as supplied. Copolymers of this sort are commonly referred to as cationic-polyacrylamides (C-PAM), which will be the case here.

3.3.2 Experimental Set-up

3.3.2.1 Set-up for measuring plug break-up pressure

The experimental apparatus used for measuring the break-up pressure of the pulp fibre plug is illustrated in Figures 3.1 and 3.2. The apparatus consisted of a modified version of the one described in Chapter 2, the key difference being the plastic column. In this work, an additional section was attached to the bottom section of the column, which allowed the initial consistency of the plug to be controlled more precisely than it was in the work of Chapter 2. The attached section contained an adjustable pipe, where the bottom of the pipe contacted the porous plate resting on top of the plug, thereby fixing the initial plug thickness. Therefore, the initial consistency of the plug could be controlled by adjusting the vertical position of the pipe.

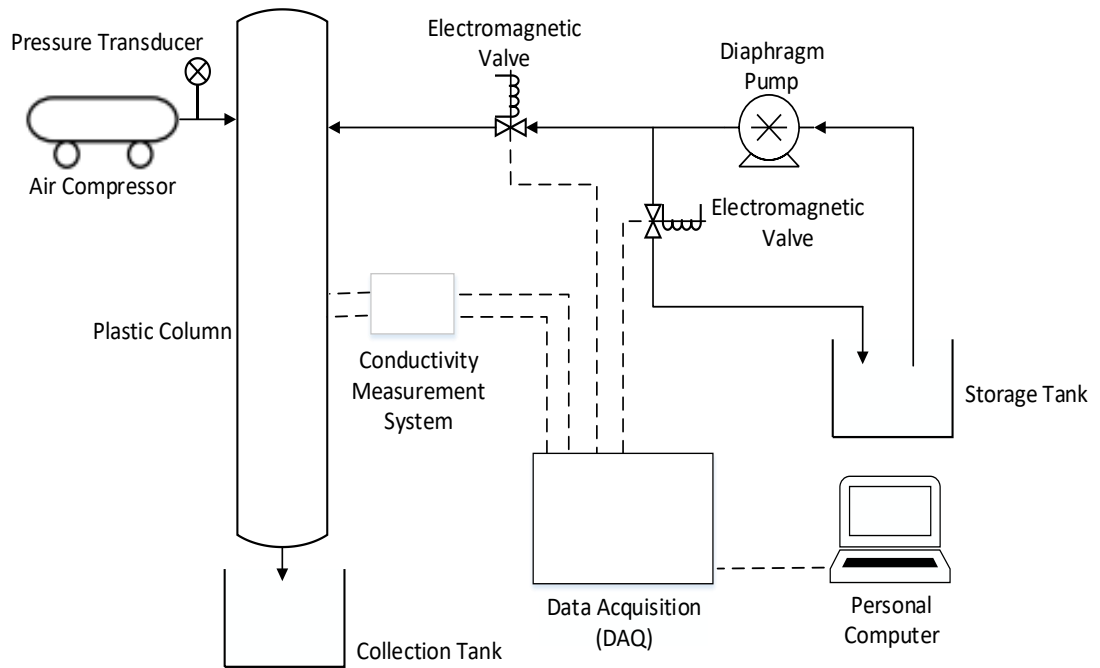


Figure 3.1. Schematic diagram of the experimental set-up for measuring the plug break-up pressure.

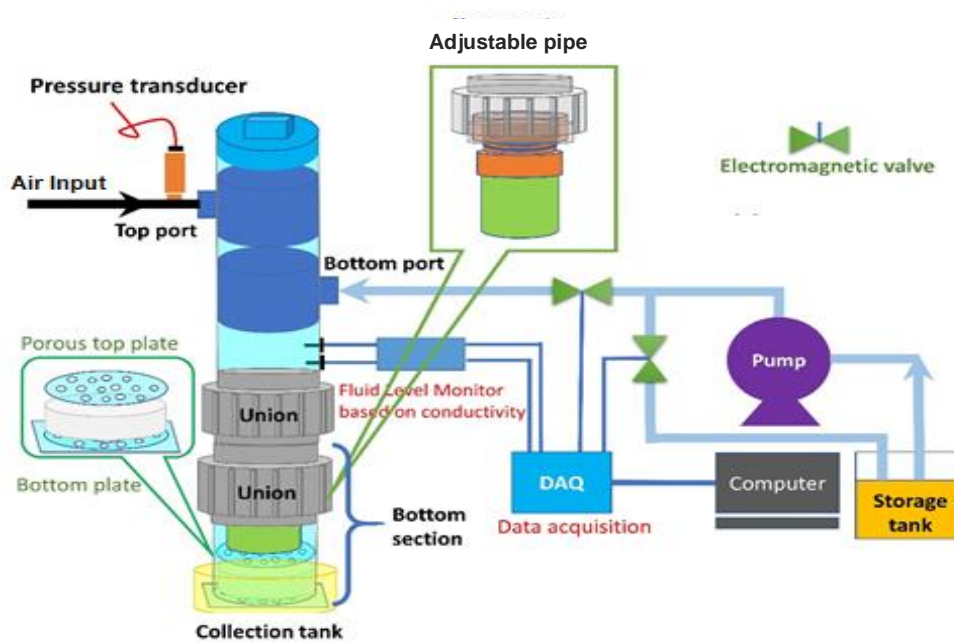


Figure 3.2. Cartoon diagram of the experimental set-up for measuring the plug break-up pressure.

3.3.2.2 Plug formation method

The method for preparing the pulp fibre plug was very similar to that which was described in Chapter 2. Unless otherwise specified, the plugs were prepared using tap water at room temperature. For the experiments described in this chapter, excess water was discarded and replaced with the operating fluid (i.e. C-PAM solution) to prevent dilution effects when filling the column with the operating fluid. The vertical position of the adjustable pipe was then set according to the desired plug thickness (or consistency) and was attached to the bottom part of the column via a union.

3.3.2.3 Break-up pressure measurement

Once the plug was formed, it was soaked with the operating fluid (tap water or C-PAM solution) by controlling the fluid level for a designated time (reaction time) and pressure. For pre-pressure treatment, the pressure within the column was controlled at a designated level (e.g. 5 psi) for a prescribed time prior to further increasing the air pressure to break the plug. All other steps involved in breaking the plug were identical to those described in Chapter 2. All break-up pressure measurements were gauge pressures (i.e. psig rather than psia).

3.3.3 Analytical Methods

3.3.3.1 C-PAM adsorption measurement

For C-PAM adsorption measurements, a 4.4 g sample (dry basis) of NBSK pulp was mixed and soaked in a C-PAM solution of known concentration for a duration of 5 minutes. The suspension was then gravity filtered and a 50-mL sample of the filtrate was collected. Since the concentration of the original C-PAM solution, the concentration of

C-PAM in the filtrate, and the solution volumes were known, the amount of C-PAM that had adsorbed onto the fibre surface during the soaking time could be estimated. The concentration of C-PAM in the solutions was determined by UV-Vis spectroscopy as described by Gibbons [80] at a wavelength of 220 nm. A standard curve was prepared, and the relationship between C-PAM concentration and absorbance was established. The coefficient of determination was 0.998.

3.4 Results and Discussion

3.4.1 Effect of C-PAM Concentration

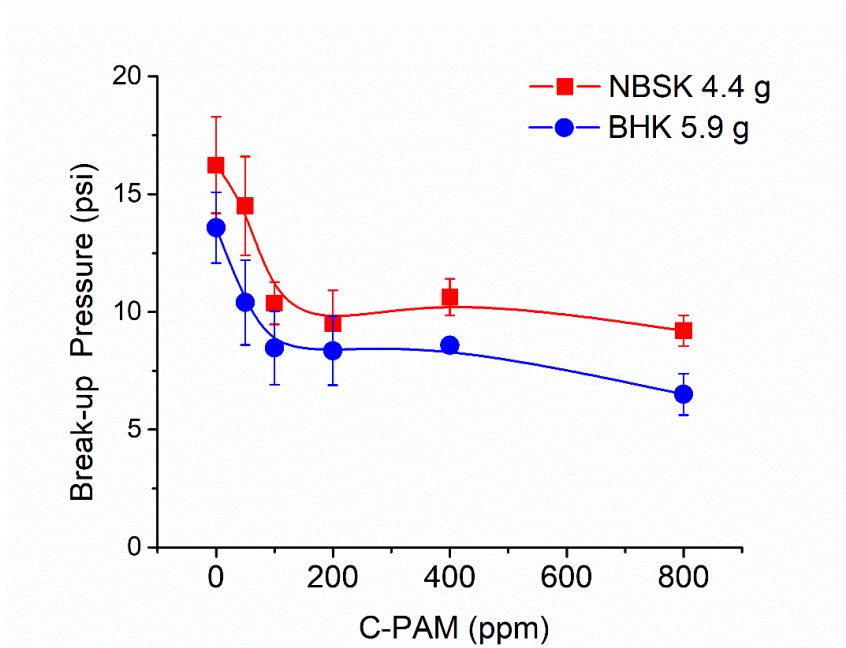


Figure 3.3. Break-up pressure for different C-PAM concentrations and pulp fibre types (initial pulp consistency: 15 wt.%; reaction time: 30 min).

Figure 3.3 demonstrates the effect of C-PAM concentration on the break-up pressure of the plug. The break-up pressure of NBSK pulp plugs has a similar trend to that of BHK pulp plugs when the concentration of the C-PAM solution is 0 – 800 ppm.

For both pulp types, the break-up pressure decreases by over 5 psi when the C-PAM concentration is increased from 0 to 100 ppm. However, when the concentration is increased to 200 or 400 ppm the break-up pressure does not continue to decrease appreciably. Additionally, when the C-PAM concentration is increased to 800 ppm, an additional decrease in break-up pressure of approximately 2 psi is observed. These results indicate that the majority of the pressure-reduction benefits are achieved at low C-PAM concentration.

The decrease in break-up pressure is attributed to be the reduction of inter-fibre friction induced by C-PAM adsorption. After a sufficient amount of C-PAM adsorbs onto the fibres, electrostatic repulsion and steric forces decrease the friction between fibre surfaces [78, 47]. As a result, a reduction in the interlocking forces between fibres occurs within the network [43, 7], thereby decreasing the break-up pressure. The adsorption of C-PAM onto the fibres may be driven by electro-steric stabilization [81]. In this case, adsorption is a dynamic process, and due to the porous nature of the fibre-based plug, the adsorption depends largely on the bulk concentration and the viscosity of the C-PAM solution, the permeability of the plug, and the pressure drop across the plug.

It is important to note that as the pressure head on the plug increases, the consistency of the plug will increase accordingly due to dewatering and compression of the plug. For this reason, all subsequent trials used an initial plug consistency of 35 wt.%, so that the effectiveness of C-PAM treatment could be assessed under lower permeability and higher consistency conditions.

To investigate the relationship between the adsorption of C-PAM onto the fibre surface and the plug break-up pressure, a modified method was used. This modification,

as described in section 3.3.3.1 was made so that the equilibrium amount of C-PAM adsorbed onto the fibre surface could be determined, given that sufficient time and mixing were provided. These samples were then used for determining C-PAM adsorption, but not for measuring the break-up pressure. The break-up pressure at the corresponding concentration was determined at an initial plug consistency of 35 wt.% and a reaction time of 30 minutes, following the procedures outlined in sections 3.3.2.2 and 3.3.2.3.

As shown in Figure 3.4, the break-up pressure is inversely related to the adsorption capacity of C-PAM onto the fibre surface. The adsorption capacity increases significantly when the C-PAM concentration is increased from 0 to 200 ppm; however, once the concentration exceeds 200 ppm, adsorption does not increase further. These findings are in general agreement with the results shown in Figure 3.3 and Figure 3.4. (break-up pressure curve), which demonstrate that the break-up pressure does not decrease significantly once the C-PAM concentration is greater than approximately 100 – 200 ppm. These results are also supported by Zauscher and Klingenberg's [47] study, in which they suggest that the effectiveness with which a polymer can reduce sliding friction between fibres is a function of the adsorbed amount of polymer.

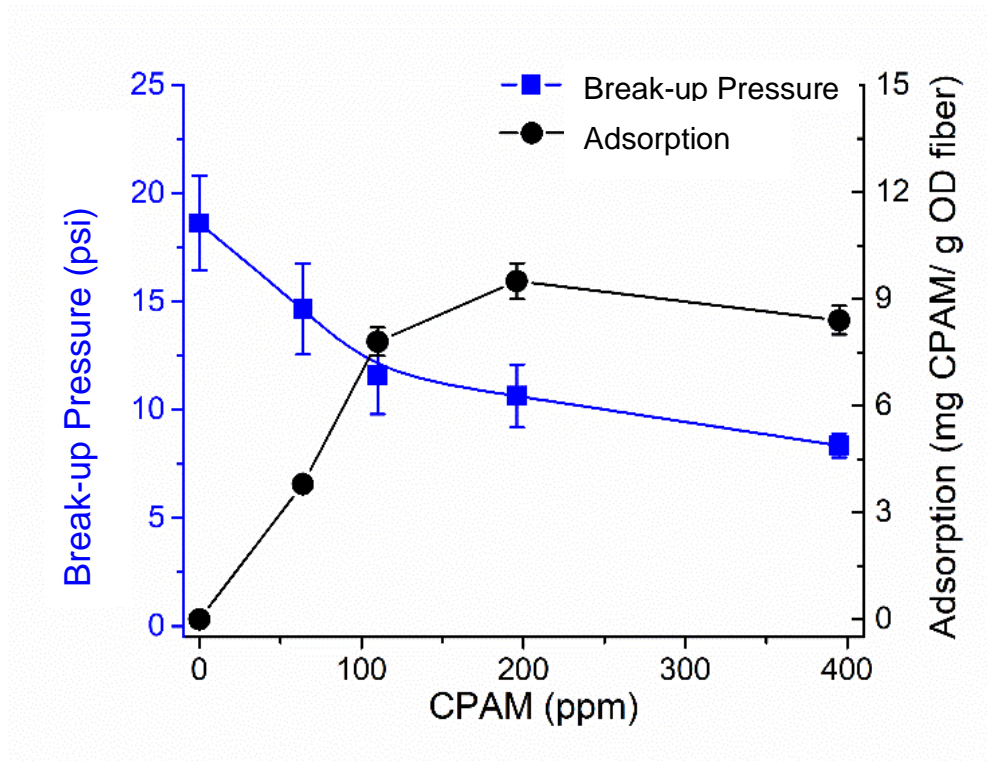


Figure 3.4. Effect of C-PAM concentration on break-up pressure and C-PAM adsorption. (initial pulp consistency: 35 wt.%; mixing time: 5 min (for adsorption measurement); reaction time: 30 min (for break-up pressure measurement)).

In this study, the effect of C-PAM molecular weight and charge density on the break-up pressure was not investigated. However, Zauscher and Klingenberg [47] have demonstrated that the C-PAM used in this study (Percol[®] 175) can reduce inter-fibre friction effectively. Therefore, since the potential for friction reduction was validated, the reduction of friction in higher pulp consistency systems, such as the case of pulp-fibre plugs, was the focus of this work. In their work, Zauscher and Klingenberg measured the molecular weight of the C-PAM as $(5.0 \pm 1.0) \times 10^6$ g/mol and the charge number density as 1.1 meq/g.

3.4.2 Effect of Reaction Time

Figure 3.4 demonstrates that adsorption begins to plateau when the C-PAM concentration is approximately 100 – 200 ppm, therefore it is of interest to investigate the effect of reaction time on the break-up pressure at these concentrations. As shown in Figure 3.5, when the reaction time is 10 or 30 minutes, the break-up pressure decreases from approximately 19 psi for the water treatment to approximately 10 psi for the 200 ppm C-PAM treatment. However, when the C-PAM concentration is 100 ppm, reaction times of 30 minutes and 10 minutes decrease the break-up pressure to approximately 9 psi and 16 psi, respectively.

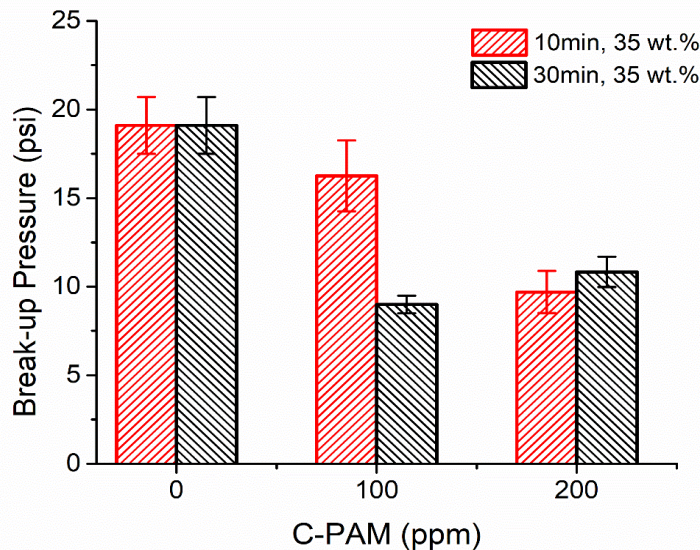


Figure 3.5. Effect of reaction time on plug break-up pressure at different C-PAM concentrations (initial pulp consistency: 35 wt.%).

These results suggest that increasing the C-PAM concentration results in an increase in the rate of polymer adsorption onto the fibre surface; a finding which is consistent with that demonstrated by Shulga et al. [82]. Therefore, to induce a similar

decrease in break-up pressure, a longer reaction time is required for the 100 ppm C-PAM treatment relative to the 200-ppm treatment, due to the rate of polymer adsorption. Consequently, a 100 ppm C-PAM solution is effective for reducing the break-up pressure, provided sufficient reaction time is allotted.

3.4.3 Effect of Pre-Pressure

For industrial applications, it is advantageous for the required reaction time to be as short as possible, thus reducing operational downtime. This section describes an alternative method for de-plugging that was implemented to decrease the time requirement for plug removal. Using this method, a 100 ppm C-PAM solution was applied to the plug, while the pressure within the column was maintained at a known value (i.e. “pre-pressure”) for a designated reaction time. Once the reaction time had elapsed, the standard plug break-up procedure was followed, as described earlier. In the case that no pre-pressure was used, the reference pressure within the column was measured as 0.3 psi.

As shown Figure 3.6, for a 10-minute reaction time and a 0.3 psi pre-pressure, the 100 ppm C-PAM treatment does not reduce the break-up pressure significantly compared to its corresponding water trial with the same conditions. However, when the pre-pressure is increased to 5 psi, and the reaction time is 5 or 10 minutes, the break-up pressure is decreased to approximately 10 psi. These results demonstrate that by applying the 100 ppm C-PAM solution to the plug under a pressurized flow of 5 psi, the required reaction time decreases from 30 minutes to as little as 5 minutes.

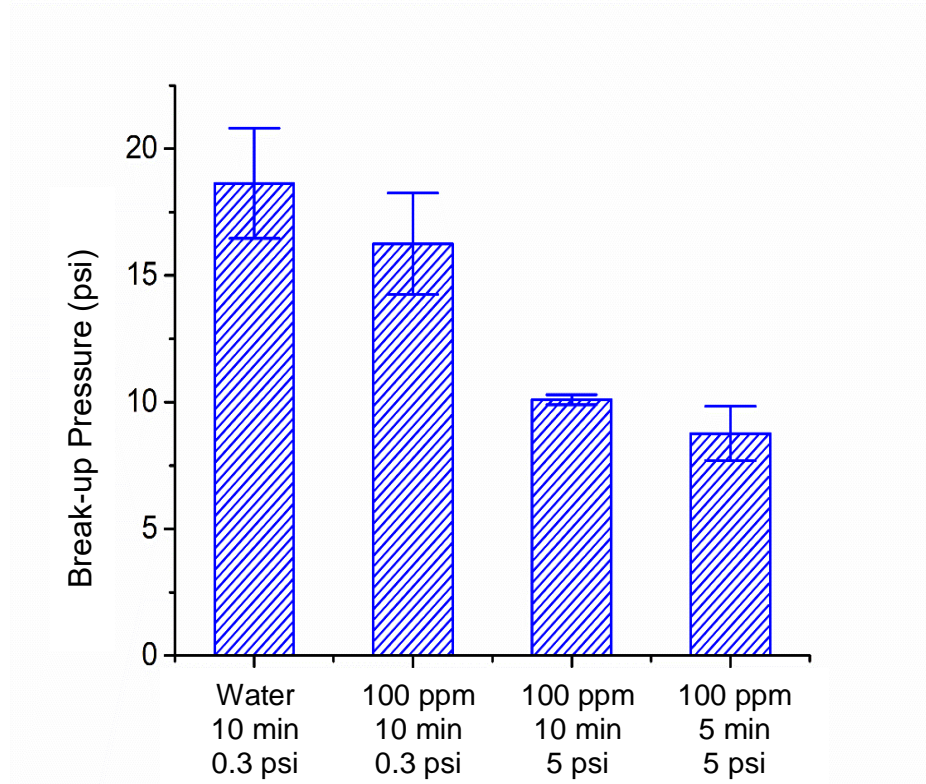


Figure 3.6. The effect of pre-pressure and reaction time on break-up pressure (initial pulp consistency: 35 wt.%).

During the de-plugging trials, it is visually apparent that the flow rate of the C-PAM solution through the plug is greater for the 5 psi pre-pressure trials than for the 0.3 psi reference trials. The decrease in break-up pressure is attributed to the increased pressure within the column, which increases the amount of polymer adsorption that occurs during the reaction time [83].

3.4.4 C-PAM Assisted De-Plugging Mechanism

C-PAM adsorbs irreversibly onto the negatively-charged surface of cellulose fibres via electrostatic interactions, in the form of ion-exchange [84]. The adsorption process occurs rapidly, in certain cases taking only 10 seconds to achieve approximately

50% of the equilibrium adsorption amount [84]. The adsorbed polymer conformation is described as a “loops-trains-tails” model, with the conformation depending on the charge density of the polymer and fibre surfaces [85]. Initially, polymers adsorb onto the fibre surface in a rather coiled conformation, with a low number of bound polymer segments (mostly loops and tails). However, with increasing time, the conformation changes, creating a flatter layer on the surface (mostly trains) [84, 81]. Additionally, due to its high molecular weight, C-PAM cannot diffuse into or through the fibre wall, and is therefore restricted to the external surface area [85, 84].

The cellulose/C-PAM system exhibits complex behaviour and is not yet clearly understood; however, some noteworthy work has been done. Mosse et al. [48] used C-PAM to decrease the yield stress of pulp suspensions, attributing the results to a combination of electrostatic and steric effects. On the other hand, Zauscher and Klingenberg [47] decreased the coefficient of sliding friction between model cellulose surfaces using C-PAM, suggesting that the decrease in friction is primarily caused by the adsorbed polymers masking fibre surface asperities, thus allowing fibres to slide past one another more easily, decreasing the network strength. The effectiveness of a polymer to mask surface asperities depends on the thickness of the adsorbed layer, which is a consequence of polymer conformation, adsorbed amount, molecular weight, and applied load.

The mechanisms described thus far rely on the fibre surfaces being readily accessible to the C-PAM solution, which is typically the case if a C-PAM solution is mixed with a pulp suspension of low consistency. However, in the case of pulp plugs, where the consistency is much greater (e.g. 15 – 35 wt.%), the properties of the plug,

such as consistency and permeability, should be considered to accurately and completely describe the adsorption phenomena. Unfortunately, there is very little work that has focused on this area.

3.5 Conclusions

C-PAM solutions of various concentrations were used to decrease the pressure head required for pulp fibre-based plug removal. In this study, a laboratory-scale set-up was used to measure the break-up pressure of pre-formed plugs, which served as an indicator for overall plug strength. The results demonstrated that a relatively low concentration C-PAM solution could be used to decrease the break-up pressure of NBSK and BHK-based plugs. The results are attributed primarily to the irreversible adsorption of C-PAM onto the fibre surfaces. Increasing the C-PAM concentration from 0 to 800 ppm resulted in the plug break-up pressure decreasing by 43% for NBSK-based plugs, and by 51% for BHK-based plugs. When the initial plug consistency was 15 wt.%, a 100 ppm C-PAM solution could significantly decrease the break-up pressure when the reaction time was 30 minutes. For plugs that have been significantly dewatered and compressed, and thus possess a higher consistency (i.e. 35 wt.%), a 100 ppm C-PAM solution under pressurized flow (5 psi) was used to reduce the required reaction time to as little as 5 minutes.

4 Conclusions and Recommendations

4.1 Conclusions

A laboratory-scale set-up was used for measuring the break-up pressure of a fibre-based plug, which was indicative of the fibre network strength. The results indicate that the break-up pressure has a power-law dependency on the plug mass when the plug mass is between 3.0 and 5.0 g. Additionally, the break-up pressure increases when the center hole diameter decreases.

CED solution was used as a chemical additive for decreasing the pressure required for plug removal. For CED concentrations of 0.04 and 0.1 M, the break-up pressure increases due to fibre swelling, which results in an increase in fibre contact area. The swelling mechanism is supported by the measured fibre properties and the water retention value. On the other hand, for CED concentrations of 0.15 and 0.2 M the break-up pressure decreases due to partial fibre dissolution, which decreases the effective fibre length, consequently decreasing the network strength. The partial fibre dissolution mechanism is supported by the measured fibre properties, the plug mass loss calculation, and the optical microscopy images.

C-PAM solution was also used for decreasing the fibre network strength, and therefore the break-up pressure. A C-PAM concentration of 100 ppm proved effective for substantially decreasing the network strength of hardwood and softwood-based plugs when the reaction time was 30 minutes and the initial solids content of the plug was 15 wt.%. Furthermore, a similar decrease in network strength could be achieved when the initial solids content of the plug was 35 wt.% by applying the C-PAM

solution under pressurized flow conditions (i.e. 5 psi) for 5 minutes. With increasing C-PAM concentration from 0 to 400 ppm, the break-up pressure decreases quickly, then levels off, while the adsorbed amount of C-PAM increases quickly then levels off. This suggests that the effectiveness with which C-PAM treatment can decrease the break-up pressure depends on the amount of C-PAM adsorbed.

4.2 Recommendations for Future Work

There are several aspects of this work that should be further investigated. First, the effectiveness with which CED and C-PAM can decrease the pressure head required for plug removal should be validated on the industrial scale, or, at a minimum, with much larger plug masses. For larger plus masses, it is likely that the required reaction time will be significantly longer, due to the greater number of fibres that need to be affected to achieve a similar decrease in network strength.

It would be beneficial to quantify the minimum required amount of de-plugging chemical on a per unit mass or volume basis of the plug. In this case, if the mass or volume of the plug is known, then the dosage requirement can be calculated directly. However, it is possible that the normalized dosage may not be constant with increasing plug mass or volume, which is another reason why this relationship should be investigated.

The mechanism through which C-PAM likely acts to decrease the fibre network strength was discussed; however, more experimental work should be done to better understand the details associated with the mechanism. Some properties that could be measured to accomplish this include but are not limited to: fibre surface charge during

the adsorption process, polymer conformation on the surface, polymer layer thickness, and fibre charge compensation due to adsorption.

References

- [1] R. J. Kerekes, R. M. Soszynski and P. Doo, "The flocculation of pulp fibres," in *8th Fundamental Research Symposium*, Oxford, England, 1985.
- [2] R. J. Kerekes and C. J. Schell, "Characterization of fibre flocculation by a crowding factor," *Journal of Pulp and Paper Science*, vol. 18, no. 1, pp. 32-38, 1992.
- [3] S. G. Mason, "The motion of fibres in flowing fluids," *Pulp and Paper Canada Magazine* 51(5), pp. 93-100, 1950.
- [4] R. M. Soszynski and R. J. Kerekes, "Elastic interlocking of nylon fibres suspended in liquid, Part 1, nature of cohesion among fibres," *Nordic Pulp and Paper Research Journal*, pp. 172-179, 1988a.
- [5] D. M. Martinez, K. Buckley, S. Jivan, A. Lindstrom, R. Thiruvengadaswamy, J. A. Olson, T. J. Ruth and R. J. Kerekes, "Characterizing the mobility of papermaking fibres during sedimentation," *Transactions of 12th fundamental research symposium, Oxford*, pp. 225-254, 2001.
- [6] R. J. Kerekes, "Pulp flocculation in decaying turbulence: a literature review," *Journal of Pulp and Paper Science* 9(3), pp. 86-91, 1983b.
- [7] C. Schmid, L. Switzer and D. Klingenberg, "Simulations of fiber flocculation: effects of fiber properties and interfiber friction," *Journal of Rheology*, vol. 44, no. 4, pp. 781-809, 2000.
- [8] D. Cheng, "Yield stress: A time-dependent property and how to measure it," *Rheologica Acta*, vol. 25, no. 5, pp. 542-554, 1986.
- [9] L. Zhu, N. Sun, K. Papadopoulos and D. De Kee, "A slotted plate device for measuring static yield stress," *Journal of Rheology*, vol. 45, no. 5, pp. 1105-1122, 2001.
- [10] C. P. Bennington, R. J. Kerekes and J. R. Grace, "The yield stress of fibre suspensions," *Canadian Journal of Chemical Engineering*, vol. 68, no. 5, pp. 748-757, 1990.
- [11] Q. D. Nguyen, T. Akroyd, D. C. De Kee and L. Zhu, "Yield stress measurements in suspensions: an inter-laboratory study," *Korea-Australia Rheology Journal*, vol. 18, no. 1, pp. 15-24, 2006.
- [12] R. Damani, R. L. Powell and N. Hagen, "Viscoelastic characterization of medium consistency pulp suspensions," *Canadian Journal of Chemical Engineering* 71 (5),

- pp. 676-685, 1993.
- [13] A. Swerin, R. L. Powell and L. Odberg, "Linear and nonlinear dynamic viscoelasticity of pulp fibre suspensions," *Nordic Pulp and Paper Research Journal* 7 (3), pp. 126-143, 1992.
- [14] C. P. Bennington, R. J. Kerekes and J. R. Grace, "Motion of pulp fibre suspensions in rotary devices," *Canadian Journal of Chemical Engineering*, vol. 69, no. 1, pp. 251-258, 1991.
- [15] B. Dalpke and R. J. Kerekes, "The influence of fibre properties on the apparent yield stress of flocculated pulp suspensions," *Journal of Pulp and Paper Science* 31 (1), pp. 39-43, 2005.
- [16] F. Ein-Mozaffari, C. J. Bennington and G. A. Dumont, "Suspension yield stress and the dynamic response of agitated pulp chests," *Chemical Engineering Science* 60 (8-9), pp. 2399-2408, 2005.
- [17] B. Derakhshandeh, S. G. Hatzikiriakos and C. P. Bennington, "The apparent yield stress of pulp fibre suspensions," *Journal of Rheology*, vol. 54, no. 5, pp. 1137-1154, 2010.
- [18] N. Thalen and D. Wahren, "Shear modulus and ultimate shear strength of some paper pulp fibre networks," *Svensk Papperstidning* 67 (11), pp. 259-264, 1964.
- [19] J. Hietaniemi and J. Gullichsen, "Flow properties of medium consistency fibre suspension," *Journal of Pulp and Paper Science* 22 (12), pp. 469-474, 1996.
- [20] A. A. Robertson and S. G. Mason, "The flow characteristics of dilute fibre suspensions," *Tappi Journal* 40 (50), pp. 326-335, 1957.
- [21] University of British Columbia Fibre Lab, "Topic 4 - Pulp Suspensions," [Online]. Available: <http://www.fibrelab.ubc.ca/files/2013/01/Topic-4-Mechanical-Pulping-Pulp-Suspension.pdf>.
- [22] G. R. Longdill and G. G. Duffy, "The shear behaviour of medium concentration wood pulp suspensions," *Appita Journal* 41 (6), pp. 456-461, 1988.
- [23] O. Luthi, "Pulp rheology applied to medium consistency pulp flow," *Proceedings of the Tappi Engineering Conference, New Orleans*, pp. 347-353, 1987.
- [24] J. A. Petterson, *Flow and Mixing of Pulp Suspensions*, Chalmers University of Technology, 2004.
- [25] Tappi, "Generalized method for determining the pipe friction loss of flowing pulp suspensions, Technical Information Paper TIP 0410-14," 2012.

- [26] M. Kufner and S. Kufner, "Micro-optics and lithography," *VUBPRESS, Brussels*, 1997.
- [27] P. Lee and W. Good, "Controlled-release technology pharmaceutical applications," American Chemical Society, Washington, DC, 1987.
- [28] R. Langer and J. Vacanti, "Artificial Organs," *Sci Am* 273 (3), pp. 130-133, 1995.
- [29] L. Szczesniak, A. Rachocki and J. Tritt-Goc, "Glass transition temperature and thermal decomposition of cellulose powder," *Cellulose* 15, pp. 445-451, 2008.
- [30] K. Ueberreiter, "The solution process," *Diffusion in Polymers, Academic Press*, pp. 219-57, 1968.
- [31] B. Miller-Chou and J. Koenig, "A review of polymer dissolution," *Progress in Polymer Science* 28, pp. 1223-1270, 2003.
- [32] J. Mercer. British Patent 13,296, 1850.
- [33] H. Chanzy and E. Roche, "Fibrous transformation of Valonia cellulose I into cellulose II," *Journal of Applied Polymer Science*, pp. Symposium 28, 701-711, 1976.
- [34] Nägeli, "Ueber den inneren Bau der vegetabilischen Zellenmembranen Sitzber," *Bay Akad Wiss Munchen*, vol. 1, pp. 282-323, 1864.
- [35] J. T. Marsh, "The growth and structure of cotton, Mercerising," Chapman & Hall, London, 1941.
- [36] C. W. Hock, "Degradation of cellulose as revealed microscopically," *Textile Research Journal*, vol. 20, pp. 141-151, 1950.
- [37] C. Cuissinat and P. Navard, "Swelling and dissolution of cellulose, Part 1: Free floating cotton and wood fibres in N-methylmorpholine-N-oxide - water mixtures," *Macromolecules Symposia*, vol. 244, no. 1, pp. 1-18, 2006.
- [38] H. Sobue, H. Kiessig and K. Hess, "The cellulose-sodium hydroxide-water system as a function of the temperature," *Z Physik Chem B*, vol. 43, pp. 309-328, 1939.
- [39] E. Schweizer, *Journal für praktische Chemie*, vol. 72, pp. 109-344, 1857.
- [40] T. Kunte and P. Kluefers, "A Transition Metal Complex of D-Glucose," *Angewandte Chemie International Edition*, vol. 40, pp. 4210-4212, 2001.
- [41] B. Arnoul-Jarriault, R. Passas, D. Lachenal and C. Chirat, "Characterization of dissolving pulp by fibre swelling in dilute cupriethylene (CUEN) solution in a

- MorFi analyser," *Holzforschung*, vol. 70, no. 7, pp. 611-617, 2016.
- [42] C. F. Schmid and D. J. Klingenberg, "Properties of Fiber Floccs with Frictional and Attractive Interfiber Forces," *Journal of Colloid and Interface Science*, vol. 226, no. 1, pp. 136-144, 2000.
- [43] L. H. Switzer and D. J. Klingenberg, "Flocculation in simulations of sheared fiber suspensions," *International Journal of Multiphase Flow*, vol. 30, no. 1, pp. 67-87, 2004.
- [44] S. R. Andersson, T. Nordstrand and A. Rasmuson, "The influence of some fibre and solution properties on pulp fibre friction," *Journal of Pulp & Paper Science*, vol. 26, no. 2, pp. 67-71, 2000.
- [45] J. R. Samaniuk, C. T. Scott, T. W. Root and D. J. Klingenberg, "Rheological modification of corn stover biomass at high solids concentrations," *Journal of Rheology*, vol. 56, no. 3, pp. 649-665, 2012.
- [46] J. Stiernstedt, Q. Zhou, T. T. Teeri and M. W. Rutland, "Friction between Cellulose Surfaces and Effect of Xyloglucan Adsorption," *Biomacromolecules*, vol. 7, no. 7, pp. 2147-2153, 2006.
- [47] S. Zauscher and D. J. Klingenberg, "Friction between cellulose surfaces measured with colloidal probe microscopy," *Colloids and Surfaces A: Physicochemical and Engineering Aspects*, vol. 178, no. 1-3, pp. 213-229, 2001.
- [48] W. K. Mosse, D. V. Boger, G. P. Simon and G. Garnier, "Effect of cationic polyacrylamides on the interactions between cellulose fibers," *Journal of Surfaces and Colloids*, vol. 28, no. 7, pp. 3641-3649, 2012.
- [49] B. Derakhshandeh, R. J. Kerekes, R. Hatzikiriakos and C. P. Bennington, "Rheology of pulp fibre suspensions: A critical review," *Chemical Engineering Science*, vol. 66, no. 15, pp. 3460-3470, 2011.
- [50] L. H. Switzer and D. J. Klingenberg, "Rheology of sheared flexible fiber suspensions via fiber-level simulations," *Journal of Rheology*, vol. 47, no. 3, pp. 759-778, 2003.
- [51] D. R. Hewitt, D. T. Paterson, N. J. Balmforth and D. M. Martinez, "Dewatering of fibre suspensions by pressure filtration," *Physics of Fluids*, vol. 28, no. 6, p. 063304, 2016.
- [52] S. Gharekhani, H. Yarmand, M. S. Goodarzi, S. F. S. Shirazi, A. Amiri, M. N. M. Zubir, K. Solangi, R. Ibrahim, S. N. Kazi and S. Wongwises, "Experimental investigation on rheological, momentum and heat transfer characteristics of flowing fiber crop suspensions," *International Communications in Heat and Mass Transfer*,

vol. 80, pp. 60-69, 2017.

- [53] F. Lundell, L. D. Söderberg and P. H. Alfredsson, "Fluid Mechanics of papermaking," *Annual Review of Fluid Mechanics*, vol. 43, pp. 195-217, 2011.
- [54] J. R. Samaniuk, C. T. Scott, T. W. Root and D. J. Klingenberg, "The influence of polymer adsorption, and fiber composition, on the rheology aqueous suspensions of aspen, cotton, and corn stover pulps," *Biomass and Bioenergy*, vol. 103, pp. 47-54, 2017.
- [55] J. R. Samaniuk, T. W. Shay, T. W. Root, D. J. Klingenberg and C. T. Scott, "A novel rheometer design for yield stress fluids," *AIChE Journal*, vol. 60, no. 4, pp. 1523-1528, 2014.
- [56] K. Moelants, R. Cardinaels, S. Buggenhout, A. M. Loey, P. Moldenaers and M. E. Hendrickx, "A Review on the Relationships between Processing, Food Structure, and Rheological Properties of Plant-Tissue-Based Food Suspensions," *Comprehensive Reviews in Food Science and Food Safety*, vol. 13, no. 3, pp. 241-260, 2014.
- [57] E. Cepeda and I. Collado, "Rheology of tomato and wheat dietary fibers in water and in suspensions of pimento purée," *Journal of Food Engineering*, vol. 134, pp. 67-73, 2014.
- [58] S. G. Advani, *Flow and rheology in polymer composites manufacturing*, Elsevier science, 1994.
- [59] W. K. Mosse, D. V. Boger and G. Garnier, "Avoiding slip in pulp suspension rheometry," *Journal of Rheology*, vol. 56, no. 6, pp. 1517-1533, 2012.
- [60] J. J. Stickel, J. S. Knutsen, M. W. Liberatore, W. Luu, D. W. Bousfield, D. J. Klingenberg, C. T. Scott, T. W. Root, M. R. Ehrhardt and T. O. Monz, "Rheology measurements of a biomass slurry: an inter-laboratory study," *Rheologica Acta*, vol. 48, no. 9, pp. 1005-1015, 2009.
- [61] J. R. Samaniuk, C. T. Scott, T. W. Root and D. J. Klingenberg, "Effects of process variables on the yield stress of rheologically modified biomass," *Rheologica Acta*, vol. 54, no. 11-12, pp. 941-949, 2015.
- [62] D. J. Klingenberg, T. W. Root, S. Burlawar, C. T. Scott, K. J. Bourne, R. Gleisner, C. Houtman and V. Subramaniam, "Rheometry of coarse biomass at high temperature and pressure," *Biomass and Bioenergy*, vol. 99, pp. 69-78, 2017.
- [63] R. Li, S. Wang, A. Lu and L. Zhang, "Dissolution of cellulose from different sources in an NaOH/urea aqueous system at low temperature," *Cellulose*, vol. 22,

no. 1, pp. 339-349, 2015.

- [64] X. Hao, W. Shen, Z. Chen, J. Zhu, L. Feng, Z. Wu, P. Wang, X. Zeng and T. Wu, "Self-assembled nanostructured cellulose prepared by a dissolution and regeneration process using phosphoric acid as a solvent," *Carbohydrate Polymers*, vol. 123, pp. 297-304, 2015.
- [65] S. Wang, A. Lu and L. Zhang, "Recent advances in regenerated cellulose materials," *Progress in Polymer Science*, vol. 53, pp. 169-206, 2016.
- [66] C. Zhang, R. Liu, J. Xiang, H. Kang, Z. Liu and Y. Huang, "Dissolution mechanism of cellulose in N, N-dimethylacetamide/lithium chloride: revisiting through molecular interactions," *The Journal of Physical Chemistry B*, vol. 118, no. 31, pp. 9507-9514, 2014.
- [67] H. -P. Fink, P. Weigel, H. Purz and J. Ganster, "Structure formation of regenerated cellulose materials from NMMO-solutions," *Progress in Polymer Science*, vol. 26, no. 9, pp. 1473-1524, 2001.
- [68] H. Wang, G. Gurau and R. D. Rogers, "Ionic liquid processing of cellulose," *Chemical Society Reviews*, vol. 41, no. 4, pp. 1519-1537, 2012.
- [69] C. Cuissinat and P. Navard, "Swelling and dissolution of cellulose Part II: free floating cotton and wood fibres in NaOH-water-additives systems," *Macromolecular Symposia*, vol. 244, no. 1, pp. 19-30, 2006.
- [70] L. Hui, Z. Liu and Y. Ni, "Characterization of high-yield pulp (HYP) by the solute exclusion technique," *Bioresource Technology*, vol. 100, no. 24, pp. 6630-6634, 2009.
- [71] B. B. Mazumder, Y. Ohtani, Z. Cheng and K. Sameshima, "Combination treatment of kenaf bast fiber for high viscosity pulp," *Journal of Wood Science*, vol. 46, no. 5, pp. 364-370, 2000.
- [72] "Viscosity of pulp (capillary viscometer method) T230 om-99," TAPPI Press, Atlanta, 1999.
- [73] E. Ott, H. M. Spurlin, M. W. Grafflin, N. M. Bikales and L. Segal, "Cellulose and cellulose derivatives," *Interscience Publishers*, vol. 5, 1954.
- [74] T. Budtova and P. Navard, "Cellulose in NaOH-water based solvents: a review," *Cellulose*, vol. 23, no. 1, pp. 5-55, 2016.
- [75] C. Cuissinat and P. Navard, "Swelling and dissolution of cellulose, Part III: plant fibres in aqueous systems," *Cellulose*, vol. 15, no. 1, pp. 67-74, 2008.

- [76] C. Cuissinat, P. Navard and T. Heinze, "Swelling and dissolution of cellulose, Part IV: free floating cotton and wood fibres in ionic liquids," *Carbohydrate Polymers*, vol. 72, no. 4, pp. 590-596, 2008.
- [77] C. Baley, "Analysis of the flax fibres tensile behaviour and analysis of the tensile stiffness increase," *Composites Part A: Applied Science and Manufacturing*, vol. 33, no. 7, pp. 939-948, 2002.
- [78] U. Raviv, S. Giasson, N. Kampf, J. Gohy, R. Jérôme and J. Klein, "Lubrication by charged polymers," *Nature*, vol. 425, pp. 163-165, 2003.
- [79] A. M. Hubbe, "Flocculation of Cellulose Fibers," *Bioresources*, vol. 2, no. 2, pp. 296-331, 2007.
- [80] M. K. Gibbons and B. Örmeci, "Quantification of polymer concentration in water using UV-vis spectroscopy," *Journal of Water Supply: Research and Technology - AQUA*, vol. 62, no. 4, pp. 205-213, 2013.
- [81] D. Solberg and L. Wågberg, "Adsorption and flocculation behaviour of cationic polyacrylamide and colloidal silica," *Colloids and Surfaces A: Physicochemical and Engineering Aspects*, vol. 219, no. 1-3, pp. 161-172, 2003.
- [82] A. Shulga, J. Widmaier, E. Pefferkorn, S. Champ and H. Auweter, "Kinetics of adsorption of polyvinylamine on cellulose fibers: I. Adsorption from salt-free solutions," *Journal of Colloid and Interface Science*, vol. 258, no. 2, pp. 219-227, 2003.
- [83] H. Butt, K. Graf and M. Kappl, *Physics and Chemistry of Interfaces*, Wiley-VCH, 2006.
- [84] L. Wagberg, L. Odberg, T. Lindstrom and R. Aksberg, "Kinetics of adsorption and ion-exchange reactions during adsorption of cationic polyelectrolytes onto cellulose fibers," *Journal of Colloid and Interface Science*, vol. 123, no. 1, pp. 287-295, 1988.
- [85] J. Su, C. J. Garvey, S. Holt, R. F. Tabor, B. Winther-Jensen, W. Batchelor and G. Garnier, "Adsorption of cationic polyacrylamide at the cellulose-liquid interface: a neutron reflectometry study," *Journal of Colloid and Interface Science*, vol. 448, pp. 88-99, 2015.

Curriculum Vitae

Ryan Mitchell Christensen

BSc (Hons), Medicinal Chemistry, University of New Brunswick, 2016

Publications:

Wen-Hui Zhang, Ryan Mitchell Christensen, Ryan Lutes, Xuesi Liu, Jinli Zhang, Mark Martinez, Harshad Pande, Bruno Marcoccia, Yonghao Ni, "Using cupriethylenediamine (CED) solution to decrease cellulose fibre network strength for removal of pulp fibre plugs", *The Canadian Journal of Chemical Engineering*, vol. 97, no. 3, pp. 662-667, 2018

Junhua Zhang, Qidi Liang, Wenxing Xie, Lincai Peng, Liang He, Zhibin He, Susmita Paul Chowdhury, Ryan Christensen, Yonghao Ni, "An Eco-Friendly Method to Get a Bio-Based Dicarboxylic Acid Monomer 2,5-Furandicarboxylic Acid and Its Application in the Synthesis of Poly(hexylene 2,5-furandicarboxylate) (PHF)", *Polymers*, vol. 11, no. 2, pp. 197-211, 2019

Conference Presentations:

Pipeline Flow of Pulp Slurries: Causes of Plugging and Possible Solutions, PAPTAC Atlantic Branch Conference, Pictou, Nova Scotia, Canada, 2017